Finanziato dall'Unione europea NextGenerationEU
Ministero dell'Università e della Ricerca
Italiadomani PIANO NAZIONALE DI RIPRESA E RESILIENZA

University of Messina

Department of Biomedical Sciences, Dental Sciences & Morpho-functional Imaging (BIOMORF)

PhD in Translational Molecular Medicine and Surgery

XXXVIII Cycle

Coordinator: Prof. Antonio Toscano

CHARACTERIZATION OF THE ENDOPHENOTYPES AND IDENTIFICATION OF NEW BIOMARKERS IN THE AUTISM SPECTRUM DISORDER

PhD student:

Giulia **SPOTO**

Tutor:

Chiar.ma Prof.ssa Daniela **CACCAMO**

Co-Tutor:

Chiar.ma Prof.ssa Gabriella **DI ROSA**

A.A. 2024/2025

Table of contents

Abstract

Background: Autism Spectrum Disorder (ASD) is a highly heterogeneous neurodevelopmental condition, characterized by wide variability in clinical presentation, developmental trajectories, and underlying biological mechanisms. This heterogeneity poses major challenges for diagnosis and stratification and suggests the involvement of complex interactions among genetic, epigenetic, metabolic, immune, and neurobiological factors.

Rationale: The identification of biologically meaningful endophenotypes may provide a refined framework for characterizing ASD beyond categorical diagnostic definitions. Integrative approaches combining molecular, peripheral, neurophysiological, and clinical data may support the identification of coherent biological patterns associated with specific developmental and behavioural profiles.

Methods: This thesis comprises four experimental studies. Study I examines genetic variants involved in oxidative stress regulation and xenobiotic metabolism. Study II investigates genome-wide DNA methylation profiles. Study III integrates clinical and neuropsychological characterization with peripheral biochemical, metabolic, inflammatory, and neurotrophic biomarkers. Study IV provides an exploratory analysis of structural brain MRI and electroencephalographic (EEG) features in relation to clinical and neurodevelopmental characteristics.

Results: Genetic variants related to redox regulation are associated with ASD, alongside alterations in oxidative stress markers. Epigenetic analyses reveal differential methylation patterns involving immune-related and neurodevelopmental pathways. Peripheral biomarker analysis highlights inter-individual variability and identifies associations with developmental and behavioural features. Neuroimaging and EEG findings are described in relation to clinical and neurodevelopmental profiles.

Conclusions: Overall, this work supports a multidimensional view of ASD, in which the integration of genetic, epigenetic, peripheral biological, neuroimaging, neurophysiological, and clinical data contributes to the identification of endophenotypic dimensions and improved stratification of the disorder.

1. Introduction

Autism Spectrum Disorder (ASD) is a neurodevelopmental condition characterized by two core features: social communication deficits and restricted, repetitive sensory-motor behaviours [1]. Over recent decades, reported prevalence has increased substantially, with current U.S. surveillance data indicating that approximately 1 in 36 children meet diagnostic criteria, and with a consistent male predominance of nearly 4:1 [2]. Although improved recognition and evolving diagnostic practices contribute to this trend, epidemiological studies indicate that these factors alone are insufficient to explain the scale of the increase [3,4].

ASD is marked by extensive clinical and biological heterogeneity, spanning cognitive, linguistic, sensory, motor, behavioural, and medical domains. This variability poses challenges for early diagnosis, prognostic stratification, and mechanistic interpretation. Historically defined through behavioural observation, ASD is now understood as the outcome of complex interactions between genetic susceptibility and environmental exposures. Large-scale sequencing efforts have identified numerous rare and de novo variants affecting synaptic development, neuronal differentiation, transcriptional regulation, and chromatin remodelling, including variants in *MECP2*, *FMR1*, *TSC1/2*, and *SHANK3* [5,6]. The list of ASD-associated genes has expanded considerably, with more than one thousand loci represented in the Simons Foundation Autism Research Initiative

(SFARI) database, many converging on pathways fundamental to neurodevelopment [7,8].

Nonetheless, genetic variation alone does not account for the full spectrum of ASD phenotypes. Increasing attention has therefore shifted toward environmental and perinatal factors that may modulate risk. Prenatal metabolic alterations have been associated with oxidative stress, mitochondrial dysfunction, neuroinflammation, and epigenetic dysregulation, each capable of influencing fetal brain development [9]. Hormonal influences, particularly those involving sex steroid pathways such as ERβ, RORA, and oxytocin signalling, have been proposed as contributors to both ASD pathophysiology and sex-biased prevalence [10,11]. Additional factors (*i.e.*, maternal infections, medication exposure, nutritional deficiencies, and air pollutants) may converge on shared pathways such as immune activation and oxidative stress, influencing neurodevelopmental vulnerability [12,13].

Many of these environmental influences exert their effects through epigenetic mechanisms, particularly DNA methylation, which plays a central role in shaping gene expression during early neurodevelopment. Epigenetic alterations have been reported in both brain tissue and peripheral blood of individuals with ASD, suggesting dynamic gene–environment interactions across multiple developmental windows [14,15]. In parallel, growing interest in peripheral biomarkers (*i.e.*, including inflammatory cytokines,

metabolic indicators, oxidative stress markers, microRNAs, and growth factors) reflects an effort to identify accessible biological signatures associated with ASD. However, despite numerous promising candidates, no single biomarker has demonstrated sufficient sensitivity or specificity for routine clinical use, and current diagnostic standards remain behaviourally based [16]. Reproducibility across studies remains limited, partly due to the intrinsic heterogeneity of ASD and methodological variability [17–19].

These challenges have led to a conceptual shift: rather than treating ASD as a single condition, current research increasingly focuses on identifying biologically meaningful endophenotypes, defined as measurable components in the pathway between genetic liability and clinical presentation [20]. Endophenotypes can reflect common molecular, neurophysiological, metabolic, or behavioural features shared by specific subgroups of individuals with ASD, independent of surface-level diagnostic categories [21]. This multidimensional perspective aligns with evidence from genetics, neuroimaging, immunology, and epigenetics, all pointing toward a need for integrative frameworks that connect biological findings with neuropsychological and developmental patterns.

Given the heterogeneity of ASD and the limitations of single-domain approaches, a comprehensive and integrative strategy is essential for capturing the biological diversity underlying the spectrum. This thesis is therefore built upon the premise that combining

neuropsychological evaluation with biochemical, metabolic, inflammatory, genetic, and epigenetic data can support the identification of biologically coherent endophenotypes and contribute to a more refined and mechanistic understanding of ASD. The following section outlines the specific rationale and objectives guiding this multidimensional investigation.

2. Rationale

The guiding premise of this thesis is that the complexity of ASD can be more accurately described when clinical and biological dimensions are examined within an integrated framework. Detailed neuropsychological characterization, considered alongside biochemical, metabolic, inflammatory, genetic, and epigenetic measures, offers the opportunity to detect patterns that are not apparent when each domain is analysed in isolation. Examining phenotypic variability in relation to markers of inflammation, oxidative stress, vitamin and metabolic status, cytokine and growth factor profiles, genetic variants, and DNA methylation signatures may facilitate the identification of biologically meaningful subgroups within the spectrum.

A further objective is to explore potential biomarkers that could support earlier detection and refined prognostic stratification. The lack of validated molecular indicators in current clinical practice highlights the need for approaches that link biological signatures with neuropsychological and developmental features. Integrating molecular data with clinical and instrumental measures may help elucidate pathways contributing to ASD heterogeneity and clarify mechanisms underlying specific endophenotypic dimensions.

Through this multidimensional strategy, the thesis aims to contribute to a biologically grounded model of ASD. By systematically combining neuropsychological, molecular, genetic, and epigenetic data, the work seeks to delineate coherent endophenotypes and

provide a foundation for future precision-oriented approaches tailored to individual neurodevelopmental profiles.

In light of this multidimensional framework, the following chapters articulate how these principles were operationalized across four complementary studies. Study I investigates genetic contributors to ASD, focusing on polymorphisms involved in oxidative stress and xenobiotic metabolism. Study II examines genome-wide DNA methylation profiles to identify epigenetic signatures and differentially enriched biological pathways. Study III integrates detailed neuropsychological characterization with peripheral biochemical, inflammatory, and neurotrophic biomarkers to explore potential clinical–biological correlations and endophenotypic patterns. Study IV provides an exploratory analysis of neuroimaging and neurophysiological features, assessing their relationship with developmental and clinical variables. Together, these studies construct a coherent, multilevel investigation aimed at capturing the biological and phenotypic heterogeneity that characterizes ASD.

3. Study I - Genetic Contributors to ASD

This chapter is based on a study that has been published as: Spoto et al. (2025). Single Nucleotide Polymorphisms in Oxidative Stress-Related Genes Are Associated with Autism Spectrum Disorders. *International journal of molecular sciences*, 26(19), 9768. https://doi.org/10.3390/ijms26199768.

3.1 *Materials and Methods for study I*

3.1.1 *Study Cohorts for study I*

One hundred six (83 M, 23 F; mean age: 7.9 ± 3.2 years) patients with ASD diagnosis were recruited among those attending the Unit of Child Neurology and Psychiatry at Polyclinic Hospital University in Messina (Italy). All the recruited subjects were diagnosed as affected by ASD on the basis of a clinical evaluation of symptoms. Individuals fulfilling DSM-V (fifth edition of Diagnostic and Statistical Manual of Mental Disorders) diagnostic criteria [22] for ASD were screened for non-syndromic autism using Magnetic Resonance Imaging (MRI), electroencephalogram (EEG), audiometry, urinary amino acids and organic acids, cytogenetic and fragile-X testing. Patients with dysmorphic features were excluded even in the absence of detectable cytogenetic alterations. Patients with sporadic seizures (*i.e.*, <1 every 6 months) were included; patients with frequent seizures or focal neurological deficits were excluded. Informed written consent to blood sampling

and anamnestic data collection was obtained from parents of all recruited individuals with ASD.

A cohort of ninety healthy subjects (63 M, 27 F; 21.2 ± 1.8 years), recruited for previous studies, was included for comparison of genotype frequencies in the local population.

3.1.2 *Genotyping by Real-Time PCR-Based Allelic Discrimination*

Genomic DNA was isolated from peripheral blood lymphocytes by Gentra Pure Gene DNA Purification System (Qiagen, Milan, Italy), according to the manufacturer's protocol. DNA quantification was carried out by spectrophotometric methods, and DNA integrity was checked by agarose gel electrophoresis. Genotyping of ASD patients and control subjects for SNPs presented in Table 1 was carried out by Real-time PCR allelic discrimination using pre-designed TaqMan SNP Genotyping assays available from Applied Biosystems (Applera Italia, Monza, Italy). Genotyping reactions were set up in a 96-well plate on a 7500HT Fast Real-Time PCR System (Applied Biosystems, Foster City, CA) and were carried out in a final volume of 10 µL containing 1× TaqMan Genotyping Master Mix, 1× TaqMan-specific assay, and 10 ng genomic DNA, using thermal cycling conditions suggested by manufacturer's protocols.

Table 3.1. Genetic variants analyzed in this study and corresponding TaqMan Assay IDs

Gene	**Single Nucleotide Polymorphism**	**TaqMan Assay ID**
CAT	-844T>C	C_7618104_10
GPx1	rs1800668	C_7912052_40
PON1	Q192R	C_2548962_20
SOD2	A16V	C_8709053_10
GSTP (variant 1A)	Ile105Val	C_3237198_20
GSTP (variant 1B)	Ala115Val	C_104961520
CYP2C9	CYP2C9*2	C_25625805_10
CYP2C9	CYP2C9*3	C_27104892_10
CYP2C19	CYP2C19*2	C_25986767_70
CYP2D6	CYP2D6*41	C_34816116_20
AHR	Arg554Lys	C_11170747_20
NAT1	-	C_1204334_50
NAT2	-	C_572770_20
UGT1A1	UGT1A1*6	C_2307598_20

3.1.3 *Genotyping by PCR and Electrophoresis of GST Deletion Variants*

The GSTM1 and GSTT1 gene deletions were examined by PCR and electrophoresis. Amplification consisted of a denaturation step at 94◦C for 4 min, annealing at 94◦C for 30 s, 64◦C for 30 s, and 72◦C for 30 s for 30 cycles, and polymerization at 72◦C for 7 min for 1 cycle. Forward and reverse primers and fragment leghts for GSTM1, GSTT1 and human albumin (used as the positive control) are reported in Table 2. Each 50-µL PCR reaction contained 5 µL of 10× PCR buffer, 5 µL of 25 mM MgCl2, 1 µL of 10 mM deoxynucleotides (ACGT), 1 µL of each primer (forward and reverse primers GSTT1 and GSTM1), 0.5 µL of forward and reverse primers for human albumin, 26.36 µL of ddH2O,

0.44 µL Taq, 1.76 µL TaqStart buffer, 0.44 µL TaqStart antibody, and 5 µL of unknown sample DNA. PCR products were visualized by agarose gel (2%) electrophoresis. This assay does not distinguish between heterozygous and homozygous presence of either gene; therefore, patients are designated either “homozygous null” or “heterozygous/homozygous present.” All plates contained blinded duplicates and positive and negative controls for quality control.

Table 3.2. Primer sequences and PCR amplicon lengths used for genotyping GSTM1, GSTT1, and ALB

Gene	**Forward primer**	**Reverse primer**	**Lenght**
GSTM1	GAACTCCCTGAAAAGCTAAAGC	GTTGGGCTCAAATATACGGTGG	215 bp
GSTT1	TTCCTTACTGGTCCTCACATCTC	TCACCGGATCATGGCCAGCA	489 bp
ALB	GCCCTCTGCTAACAAGTCCTAC	GCCCTAAAAAGAAAATCGCCAATC	351 bp

3.1.4 *Assessment of Oxidative Stress Levels*

In order to evaluate oxidative stress levels in ASD patients having different genetic backgrounds, the measurement of the derivatives of reactive oxygen metabolites (dROMs), the Biological Antioxidant Potential (BAP), and the advanced oxidation protein products (AOPP) were performed. We selected dROMs, AOPP, and BAP to capture complementary aspects of systemic oxidative balance, reflecting global oxidative burden, protein oxidation, and overall non-enzymatic antioxidant capacity, respectively. The dROM test and BAP test were carried out according to the manufacturer’s protocol

(Diacron International, Grosseto, Italy). dROMs reflect the amount of organic hydroperoxides that are related to the free radicals from which they are formed. The results are expressed in arbitrary units (Carratelli units), one unit of which corresponds to 0.8 mg/L of hydrogen peroxide.

The BAP test provides an estimate of the global antioxidant capacity of blood plasma, measured as its reducing potential against ferric ions. The results are expressed in µmol/L of the reduced ferric ions.

The measurement of AOPP serum levels was performed using a colorimetric method involving chloramine T as a standard, as described by Alazoglu et al. [23]. The assay was carried out in a 96-well microplate and sample absorbance was determined using a Sunrise microplate reader (Tecan Italia, Vernusco sul Naviglio, Milan, Italy).

3.1.5 *Assessment of Oxidative DNA Damage by Single Cell Gel Electrophoresis (Comet Assay)*

The single cell gel electrophoresis (SCGE), is a sensitive technique for quantifying and analyzing oxidative DNA damage in individual cells [24,25]. Lymphocytes were isolated from 3 mL of blood samples through the use of Histopaque 1077 (Sigma-Aldrich, Milan, Italy), resuspended with Low Melting Agar and spotted on a slide. The slides were placed in an electrophoretic pan and subjected to electrophoresis at 300 mA for 30 min in the

dark. Ethidium bromide, an intercalating agent for nucleic acid stain, was used as a dye for all slides. After 24 h samples were analyzed by the use of a Leica microscope and images were analyzed by CASP software 1.2.2., as reported by Gugliandolo et al. [26]. The parameters analyzed were Head Length, Tail Length, Comet Length, Head DNA and Tail DNA amount.

3.1.6 *Statistical Analysis*

Continuous variables were analyzed using unpaired Student's t-test, while categorical variables and compliance of allele distribution to the Hardy–Weinberg equilibrium were evaluated by Fisher's exact test. Statistically different effects of gene polymorphisms on biochemical variables were evaluated by a one-way analysis of variance (ANOVA) followed by the Newman-Keuls post hoc test. Significant values were assessed according to $p < 0.05$. All the analyses were carried out using IBM SPSS statistic v22.

3.2 *Results*

3.2.1 *Genotyping for SNPs in Antioxidant Defense Enzymes*

Individuals with ASD and controls were genotyped for the SNPs Superoxide Dismutase 2 (SOD2) A16V, Catalase (CAT) -844 C>T, Glutathione peroxidase 1 (GPx1) rs1800668, and Paraoxonase 1 (PON1) Q192R.

Genotype frequencies for the SNP SOD2 A16V were found to be in Hardy–Weinberg equilibrium both in patients and controls. The most frequent genotype in ASD group was the heterozygous AV, while the mutated variant V was more frequent in controls than in ASD group.

Genotype frequencies for the SNP CAT -844 C>T were in Hardy–Weinberg equilibrium in individuals with ASD and controls. Wild-type genotype was more common in controls compared to ASD, with a prevalence around 70%. Heterozygous genotype was statistically significant higher in patients than in controls. Neither affected individuals nor the controls resulted carriers of the homozygous mutated genotype TT.

Results from allelic discrimination for the SNP GPx1 rs1800668 showed that the frequencies were in Hardy–Weinberg equilibrium, both in patients and controls. The frequency of wild-type genotype was significantly higher in controls, while the homozygous mutated genotype was observed only in individuals with ASD. Notably, Odds Ratio (OR) calculation showed that the mutated genotype was associated with a 23 times higher risk to develop ASD (Table 3).

The distributions of genotypes for the SNP PON1 Q192R in ASD patients and controls were in Hardy-Weinberg equilibrium.

The frequency of wild-type genotype was significantly higher in healthy controls than in cases, while the homozygous mutated genotype was only observed in individuals with

ASD, and was associated with a 31 times higher risk for the disease. On the contrary, the QQ wild-type genotype resulted to be protective against ASD and associated with a two times lower risk for the disease (Table 3).

Table 3.3. Distribution of gene polymorphisms of antioxidant enzymes in ASD patients and healthy controls

Genotype	**ASD (n=106) %**	**Controls (n=90) %**	**p-value**	**Odds Ratio (95% C.I.)**
SOD2 A16V				
AA	33.02	21.11	0.0777	-
AV	36.79	26.67	0.1671	-
VV	30.19	52.22	**0.0021**	0.3956 (0.2202 to 0.7107)
CAT -844C>T				
CC	53.77	68.89	**0.0398**	0.5253 (0.2920 to 0.9453)
CT	46.23	31.11	**0.0398**	1.904 (1.058 to 3.425)
TT	-	-		-
GPx1 rs180668 C>T				
CC	54.81	75	**0.0028**	0.3924 (0.2118 to 0.7270)
CT	34.62	25	0.1569	-
TT	10.58	0	**0.001**	22.26 (1.292 to 383.6)
PON Q192R T>C				

TT	47.62	63.33	**0.0471**	0.5263 (0.2871 to 0.9649)
TC	38.10	36.67	0.8763	-
CC	14.29	0.00	**0.0001**	31.21 (1.816 to 536.4)

3.2.2 *Genotyping of polymorphisms in enzymes and proteins involved in xenobiotic metabolism*

ASD patients and healthy individuals were genotyped for the cytochrome P450 (CYP), family 2, subfamily C, polypeptide 9 and 19, and subfamily D, polypeptide 6, namely SNPs CYP2C9*2, CYP2C9*3, CYP2C19*2, CYP2D6*41 of phase I drug metabolism enzymes CYP2C9, CYP2C19, CYP2D6, the SNP Arg554Lys of the xenobiotic sensor aryl hydrocarbon receptor (AHR), and the SNPs Arg187Gln, rs179993, * 6, I104V as well as A114V of the phase II drug metabolism enzymes N-acetyl transferases (NATs), UDP-glucuronosyl transferases (UGTs), glutathione-S-transferases (GSTs): NAT1, NAT2, UGT1A1, GSTP1, respectively. Moreover, the distribution of deletion variants of the phase II drug metabolism enzymes GSTM1 and GSTT1 was also assessed in both groups. Genotype distributions for CYP2C9*2 and *3 polymorphisms were in Har-dy-Weinberg equilibrium in both patients and controls.

The CYP2C9*1/*1 wild-type genotype was the most frequent in both groups, with a higher but not significant frequency in control group. The mutated *1/*2 was more frequent among healthy controls than among cases, even if these differences was not statistically significant. The homozygous mutated *2/*2 genotype showed a very low frequency in both groups. Notably, the mutated heterozygous *1/*3 genotype was sig-nificantly more frequent in ASD patients than in healthy subjects and was associated with a 20 times increased risk for the disease (Table 2). The mutated homozygous *3/*3 gen-otype was not observed in both groups.

Genotype distribution for the CYP2C19 *2 polymorphism agreed with Har-dy-Weinberg equilibrium both in patients and controls.

The wild-type *1/*1 genotype was more frequent among healthy subjects than among ASD patients, while the mutated heterozygous *1/*2 and homozygous *2/*2 genotypes were more frequent in cases than in controls. However, these differences were not statistically significant (Table 4).

Genotype distribution for the CYP2D6*41 polymorphism was in agreement with Hardy-Weinberg equilibrium. The wild-type *1/*1 genotype was the most frequent in both groups, with a significantly higher frequency among controls, that resulted in a reduction of the risk for the disease by 53 times. The *41 mutated allele was only found in ASD

group, with the highest frequency of the heterozygous *1/*41 genotype, that was associated with a 44 times increased risk for the disease.

Genotyping for AHR Arg554Lys polymorphism showed that the genotype frequencies were in Hardy-Weinberg equilibrium. The wild-type Arg/Arg genotype was the most frequent in both groups, with a higher frequency in ASD patients. However, this difference was not statistically significant. The heterozygous mutated Arg/Lys genotype showed a similar frequency between the two groups, while the homozygous mutated Lys/Lys genotype was only found in control group.

The genotype distributions for the SNP NAT1 Arg187Gln and NAT2 was in agreement with Hardy-Weinberg equilibrium both in patients and controls. Genotype distributions were similar between the two groups, with the wild-type Arg/Arg genotype being the most represented and the heterozygous Arg/Gln genotype showing a very low frequency. The homozygous genotype was not observed (Table 4).

The distribution of the SNP NAT2 rs1799931 G>A was in Hardy-Weinberg equilibrium in both groups. The wild-type GG genotype was the most frequent in both groups. The heterozygous GA genotype was found with a very low frequency only in the control group, while the homozygous mutated AA was not observed.

The distributions of the UGT1A1 genotypes were in Hardy-Weinberg equilibrium in both groups. Results showed that the heterozygous genotype was present only in controls but

not in ASD patients, with a protective effect. We found the homozygous genotype only in individuals with ASD, with an OR of 24 times.

Genotyping results for the variants *A (Ile105Val) and *B (A114V) of GSTP1, deleted/null of GSTM1, and deleted/null of GSTT1 (deletion) showed that the genotype distributions were in agreement with Hardy-Weinberg equilibrium in both groups.

The high diversity of the genotypes determined a fragmentation of the results; the different haplotypes of GSTP1, resulting from the different combinations of the alleles *A (I105V) and *B (A114V), were grouped and their distribution was analyzed as a sum of the frequencies

The results showed a significantly higher frequency of the wild-type genotype in the control group than in ASD patients (Table 4). Instead, mutated heterozygous and homozygous genotypes were more frequent in ASD patients than in controls, even if these differences were not significant likely because of the small number of subjects included in the subgroups corresponding to different GSTP1 genotypes (Table 4). The sum of homozygous genotypes I105/A114A, homozygous/heterozygous V105V/A114A, homozygous/homozygous V105V/V114V, heterozygous/homozygous I105V/V114V and homozygous I105V/V114V had a higher frequency in patients, but these differences were not significant.

Individuals with I105V/A114V genotype had a higher frequency in controls, but also in this case there were not statistically significant differences.

Analysis of the deletion *M1 for GST revealed no differences between controls and patients.

On the contrary, analysis of the deletion *T1 for GST revealed important statistically significant differences between controls and patients. In fact, the deleted genotype was more frequent in the latter group, and it was associated with the pathology with an OR of 2.5. In controls the not deleted genotype was more common.

The frequency of subjects that had both deletions was higher in patients than controls, and this difference was statistically significant.

Table 3.4. Distribution of gene polymorphisms in phase I and II xenobiotic metabolism enzymes

Genotype	**ASD % (n=106)**	**Controls % (n=90)**	**p-value**	**Odds Ratio (95% C.I.)**
*CYP2C9*2, *3* [a]				
*1/1	73.3	84.4	0.0524	-
*1/*2	6.7	12.2	0.1058	-
*1/*3	18.3	1.1	**0.0011**	18.88 (2.236-159.4)
*2/*2	1.7	2.2	1	-
*CYP2C19*2* [b]				
*1/*1	73.91	80.0	0.445	-
*1/*2	21.74	16.7	0.4228	-
*2/*2	4.35	3.33	1	-
*CYP2D6*41* [c]				
*1/*1	77.5	100	**<0.0001**	0.01878

				(0.001-0.340)
*1/*41	20	-	**0.0002**	44.4 (2.420-814.6)
*41/*41	2.5	-	0.2623	-
AHR Arg254Lys [d]				
Arg/Arg	83.9	77.8	0.4109	-
Arg/Lys	16.1	16.7	1	-
Lys/Lys	-	5.5	0.0797	-
NAT 1 Arg187Gln [f]				
Arg/Arg	97.26	96.67	1	-
Arg/Gln	2.74	3.33	1	-
Gln/Gln	-	-	-	-
NAT 2 rs1799931 G>A [g]				
G/G	100	96.67	0.2466	-
G/A	-	3.33	0.2466	-
A/A	-	-	-	-
*UGT1A1*6 G>A*				
WT 1/1 G/G	89.09	85.56	0.6191	
ET *1/*6 G/A	-	14.44	**0.0019**	0.05172 (0.003-0.889)
OMO *6/*6 A/A	10.91	-	**0.0025**	23.77 (1.310-431.1)
GSTP1 I105V/A114V				
*A/*A	45.2	62.2	**0.024**	0.5025 (0.283 - 0.891)
*A/*B	34.5	28.9	0.5378	-
*B/*B	8.3	4.4	0.3888	-
*A/*C	4.8	2.2	0.4558	-
*A/*D	1.2	-	1	-
*B/*C	5.9	2.2	0.2923	-
GSTM1 Null (*0) [e]				
*1/*1+*1/*0	58.8	53.3	0.1494	-

*0/*0	41.2	46.7	0.1494	-
*GSTT1 Null (*0)* [e]				
*1/*1+*1/*0	64.7	80	**0.0296**	0.43 (0.210-0.878)
*0/*0	35.3	20	**0.0296**	2.326 (1.139-4.750)
GSTM1 Null/GSTT1 Null [e]				
(*1/*1+*1/*0)/ (*1/*1+*1/*0)	38.2	47	0.615	-
(*1/*1+*1/*0)/*0/*0	16.2	15.5	0.915	-
*0/*0/(*1/*1+*1/*0)	22.05	33.3	0.12	-
(*0/*0)/(*0/*0)	19.1	4.44	**0.0032**	5.000 (1.64-15.24)

Legend: [a] ASD examined were 60; [b] ASD examined were 70; [c] ASD examined were 40; [d] ASD examined were 62; [e] ASD examined were 68; [f] ASD examined were 73; [g] ASD examined were 84; [h] ASD examined were 55. GSTP1*A = I105/A114; GSTP1*B = V105/A114; GSTP1*C = V105/V114; GSTP1 *D =I105/V114

3.2.3 *Evaluation of oxidative stress markers*

The measurements of oxidative stress markers, namely dROMs, AOPP and BAP, showed that the mean values of concentration in affected individuals were higher than in controls (Table 5). These data indicated a mild oxidative stress status. These differences were significant for AOPP, with a p value <0.0001. dROMs and BAPs values were similar in controls and patients.

Table 3.5. Assessment of oxidative stress marker in ASD patients and case controls

Redox marker	ASD (n=106)	Controls (n=90)
AOPP	329.1± 149.7	74.9 ± 15.1
dROMs	327.1± 115.9	319.3 ± 50.1
BAP	2428.0± 1479.3	2128.4 ± 1820.6

Legend: Values are provided as mean ± standard deviation

We further analyzed the variability of oxidative stress markers in ASD patients having different genotypes. In particular, the study cohort was divided in three groups: 1) carriers of SOD2 wild-type genotype and several other SNPs among those examined in this study (total number of mutated alleles = 2-9), 2) carriers of SOD2 A16V heterozygous genotypes and several other SNPs among those examined in this study (total number of mutated alleles: 2-6); 3) carriers of SOD2 A16V mutated genotype and several other SNPs among those examined in this study (total number of mutated alleles = 2-6). In the comparison between the different groups, the heterozygous patients showed lower mean levels of AOPP and dROMs, and the highest mean BAP. On the contrary, the homozygous group showed the highest mean levels of AOPP and dROMs, while the lowest mean BAP was found in the wild-type group (Table 6). However, a significant difference was only observed in the BAP among the wild-type group and the patients carrying the SOD2 A16V heterozygous genotype ($p = 0.006$). Moreover, the BAP of the wild-type group showed a significant difference in comparison with the heterozygous and homozygous groups ($p = 0.004$).

Table 3.6. Variability of oxidative stress markers in ASD patients having different genotypes

	AOPP	**dROMs**	**BAP**
Group 1 (SOD2 Wt + 2-9 other SNPs) (n=35)	312.2 ± 111.9	357.3 ± 107.0	1694.0 ± 1061.9
Group 2 (SOD2 Ht + 2-6 other SNPs) (n=39)	303.0 ± 134.3	347.3 ± 101.6	3008.8 ± 1396.2
Group 3 (SOD2 Mut + 2-6 other SNPs) (n=32)	378.4 ± 151.0	401.7 ± 160.4	2392.5 ±1248.5

Legend: Values are provided as mean ± standard deviation

3.2.4 *Comet Assay DNA Damage*

The microscopical observation of lymphocytes subjected to Comet assay revealed a higher level of DNA damage in nuclei of lymphocytes isolated from ASD patients compared with healthy controls (Figure 3.1). Moreover, the measurement of comet parameters showed that there were significant differences between healthy controls and individuals with ASD (Table 3.7).

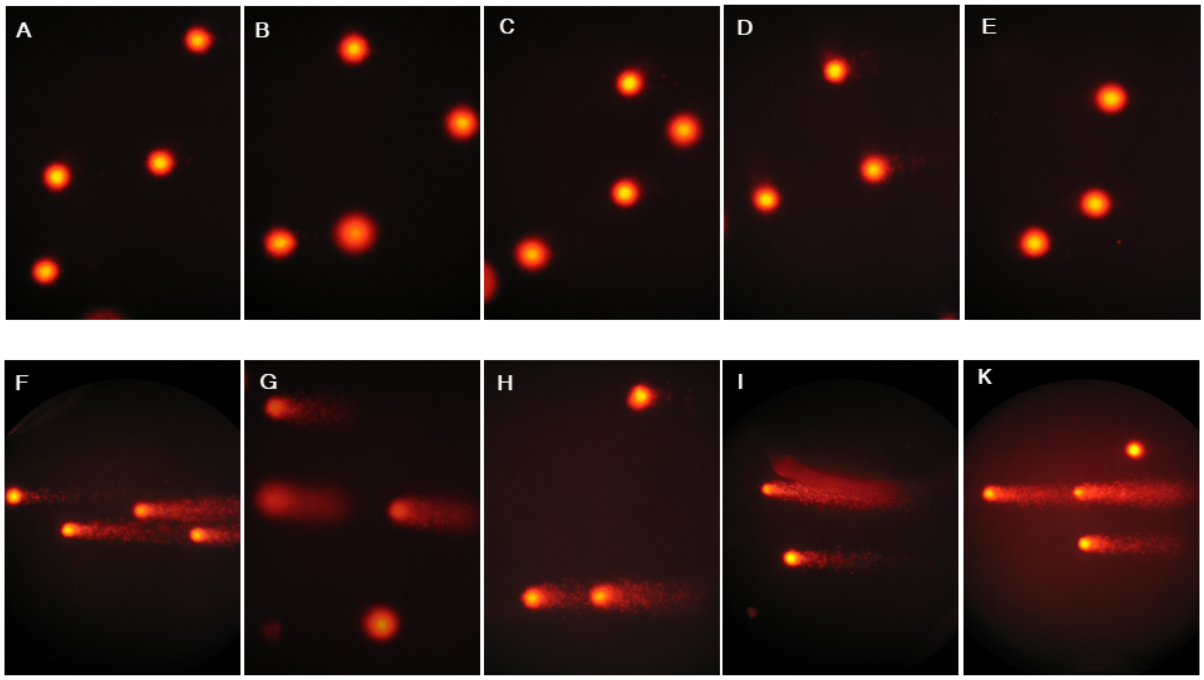

Figure 3.1. Representative images of the lymphocytes analyzed by the SCGE (Comet assay). A-E, microscope image in 5 control subjects; F-K: SCGE microscope image in 5 ASD patients.

Table 3.7. Variability of Comet $^{+}$ cells and variability of comet parameters in ASD patients and controls

Comet parameters	**ASD (n=32)**	**Controls (n=27)**
% COMET + cells	5.54 ± 4.66	4.5 ± 2.9
Head length	215.8 ± 15.3	209.5 ± 15.7
Tail length	64.5 ± 14.1	36.6 ± 9.5
Comet length	274.0 ± 20.3	252.5 ± 13.6
Head DNA	85.9 ± 4.5	112.4 ± 101.9
Tail DNA	14.04 ± 4.6	11.6 ± 4.1
Tail Moment	14.8 ± 9.8	9.3 ± 6.4
Olive Tail Moment	11.2 ± 6.2	4.0 ± 2.4

Legend: Values are provided as mean ± standard deviation

4. Study II - Epigenetic Contributors to ASD

4.1 Materials and Methods for study II

4.1.1 *Study Cohorts for study II*

The study included 44 children with a confirmed diagnosis of ASD (37 M and 6 F; mean age: 7.13 ± 3.53 years) and 10 typically developing controls (4 M and 6 F; mean age: 6.71 ± 3.45 years).

The participants were recruited partly (n = 20) at the Unit of Child Neurology and Psychiatry at Polyclinic Hospital University in Messina (Italy) and partly through a collaborating clinical site in Morocco (n = 24). All the recruited subjects were diagnosed as affected by ASD on the basis of a clinical evaluation of symptoms. Informed written consent to blood sampling and anamnestic data collection was obtained from parents of all recruited individuals with ASD.

4.1.2 *DNA Extraction*

For DNA extraction, frozen blood samples were used. Extraction was performed using the PureLink® Genomic Lysis/Binding Buffer kit (Thermo Scientific, MA, USA) to obtain blood lysates. Proteinase K and RNase A were added to each sample to ensure degradation of proteins and RNA, along with PureLink® Genomic Lysis/Binding Buffer for cell and nuclear lysis. This was followed by the DNA binding phase to columns using 96-100% ethanol,

preceded by incubation at 55°C for 10 minutes to promote protein digestion. For purification and elution steps, PureLink® Spin Columns were used. DNA elution was performed using PureLink® Genomic Elution Buffer, ultimately yielding purified DNA. The purity and quantity of the extracted DNA were assessed using a NanoDrop™ (Thermo Scientific, MA, USA) and a Qubit 4 Fluorometer (Thermo Scientific, MA, USA).

4.1.3 *Bisulfite Conversion*

For the experiment, bisulfite conversion of the extracted DNA was necessary. This step was performed using the EZ-96 DNA Methylation-Lightning™ MagPrep kit (Zymo Research Corp., CA, USA). To 250 ng of DNA, Lightning Conversion Reagent was added to facilitate the conversion of unmethylated cytosines to uracils, following DNA denaturation. Subsequently, the addition of M-Binding Buffer and EZ-Methylation Magprep Beads allowed the binding of the converted DNA strands to the beads for subsequent purification and desulfonation, which is essential to stabilize the conversion. For these final steps, M-Wash Buffer and L-Desulphonation Buffer were used. Following desulfonation, an additional wash was performed, and then a step at 55°C for 20-30 minutes was carried out to dry the beads and remove any residual M-Wash Buffer. Finally, the samples were eluted by adding M-Elution Buffer, followed by removal of the supernatant containing the DNA to be used for subsequent analysis.

4.1.4 *Array Hybridization*

The array hybridization phase was performed using the Infinium HD Methylation protocol for the Infinium MethylationEPIC v2.0 array (Illumina). The bisulfite-converted DNA samples were added to a 96-well MSA4 plate, where MA1, 0.1 N NaOH, RPM, and MSM were added and incubated in an Illumina Hybridization Oven for 20-24 hours at 37°C to allow DNA amplification. Enzymatic fragmentation of the DNA was then performed by adding FMS, followed by incubation for 1 hour in a Hybex thermoblock preheated to 37°C. For DNA precipitation, 100% 2-propanol and PM1 were used. After precipitation, the DNA samples were resuspended by adding RA1 and incubated in an oven for 1 hour at 48°C. At this point in the protocol, each sample, previously denatured at 95°C for 20 minutes, was hybridized to specific sections of the BeadChip provided in the kit. The BeadChips were then loaded into the Hybridization Chamber and incubated at 48°C for 20-24 hours. Subsequently, washes of the BeadChips were performed using PB1 to remove non-hybridized or non-specifically hybridized DNA. Following this, an extension of the primers hybridized with the samples was carried out by adding RA1, XC1, XC2, TEM, 95% formamide/1 mM EDTA, and XC3. This was followed by staining of the BeadChips, performed by adding STM, XC3, and ATM. At this point, a wash of the BeadChips was performed, followed by coating with XC4. Finally, the BeadChips were analyzed using a NextSeq 550 instrument.

4.1.5 *Bioinformatics Analysis*

To perform the bioinformatics analysis of the data obtained from the BeadChips, several steps were executed, including data quality assessment, preprocessing, normalization, and differential analysis, using R version 4.5.1, to identify differences in methylation profiles between the samples from patients with autism spectrum disorder and the examined controls. Sample quality was validated using Illumina GenomeStudio software. The obtained IDAT files were imported into minfi using the read.metharray.exp function to generate an RGChannelSet object, where sample names were assigned from the metadata sheet. An additional quality control parameter used was the p-value, through which poor-quality samples were excluded. A further control was performed on sex prediction by comparing the average methylation levels of probes on the X and Y chromosomes. Normalization was then performed, also using the minfi package, by applying functional normalization, thereby utilizing the control probes on the array to adjust methylation values. Finally, a series of standard quality control filters were applied to the probe-level data. This process involved removing probes with a high detection p-value, excluding those associated with SNPs or with a low bead count, and filtering out known cross-reactive probes.

Following the quality analysis of the BeadChips, the methylation profiles of the samples were examined. Subsequently, a differential analysis was performed to identify CpG sites and genomic regions with statistically significant methylation differences between the case samples and controls. Using the limma package, a linear modeling approach was employed to test individual CpG sites for association with the sample groups, while also performing annotation. P-value correction was performed using the Benjamini-Hochberg method, and significantly differentially methylated positions (DMPs) were identified using a false discovery rate (FDR) threshold of < 0.05. Following the DMP analysis, DMR (Differentially Methylated Region) analysis was performed using the DMRcate package to identify broader genomic regions exhibiting coherent differential methylation with greater potential biological relevance compared to individual CpG sites. This regional analysis also used an FDR threshold of < 0.05 for significance.

4.1.6 *Functional Enrichment Analysis*

Functional annotation was performed using GREAT (Genomic Regions Enrichment of Annotations Tool), version 4.0. Regions were associated with genes using the “Basal plus extension” model with default parameters. Enrichment was evaluated across Gene Ontology (GO) Biological Processes and curated pathway databases using GREAT’s

combined binomial and hypergeometric statistical framework, with FDR < 0.05 considered significant.

Hypermethylated and hypomethylated DMRs were analyzed separately. A secondary analysis was conducted by restricting DMRs to those mapped to genes listed in the SFARI Gene database, in order to assess whether ASD risk genes displayed distinct functional enrichment patterns relative to the whole DMR set.

4.2 *Results*

4.2.1 *Data Quality Control and Technical Validation*

Prior to biological interpretation, rigorous quality control and normalization were performed to ensure the integrity of the methylation data. All samples, both ASD cases and controls, passed the fundamental quality metrics, indicating successful hybridization and scanning with no critical failures. Following this, initial raw data exhibited the expected bimodal distribution but with misaligned density curves across samples, indicative of non-biological technical variation. Application of functional normalization successfully corrected for these batch effects, resulting in perfectly aligned density profiles and confirming the removal of systematic noise (Figure 4.1).

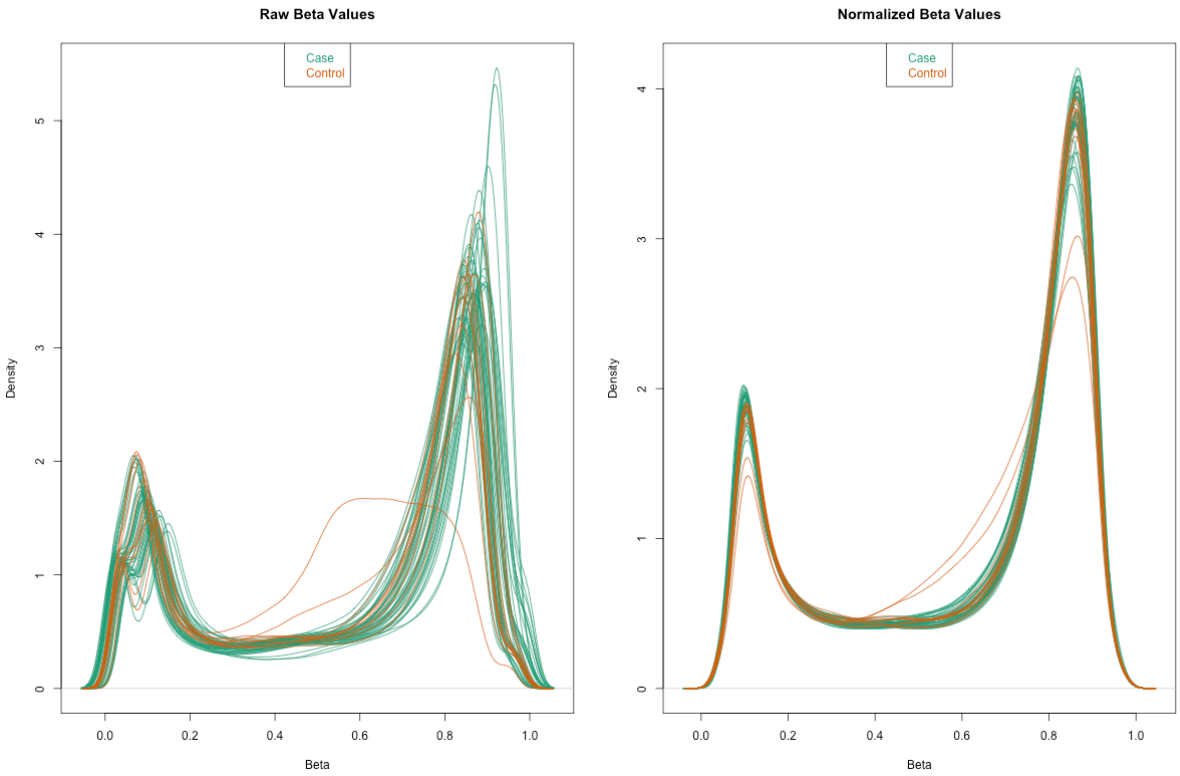

Figure 4.1. a) Density Plot of Beta Values before normalization; b) Density Plot after normalization.

Hierarchical clustering analysis of the filtered methylation profiles resulted in two primary dendrogram branches, broadly separating ASD cases from healthy controls. The control samples clustered coherently, demonstrating intra-group homogeneity. The ASD cases formed defined sub-clusters, capturing the shared epigenetic signature of the condition while reflecting its known heterogeneity. A small number of samples appeared as outliers, which is not uncommon in neurodevelopmental cohorts. This analysis confirms that diagnostic status is the primary source of epigenetic variation in the dataset (Figure 4.2).

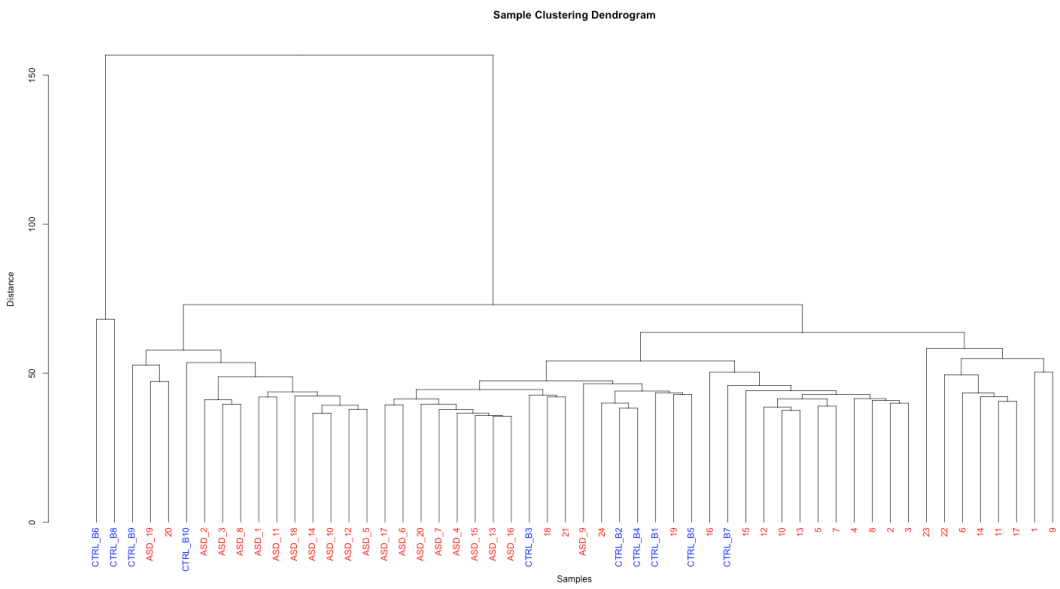

Figure 4.2. Dendrogram showing the clustering of case studies (red) and controls (blue).

4.2.2 *Differential Methylation Analysis*

The analysis progressed to a genome-wide scan to identify individual CpG sites differentially methylated in ASD. As shown in Figure 4.3, this scan revealed widespread and significant epigenetic alterations, with a substantial number of sites surpassing the significance threshold ($-\log_{10}(P) > 5$). The distribution of these Differentially Methylated Positions (DMPs) was not uniform across the genome. Instead, significant peaks were notably concentrated on specific chromosomes, including 1, 12, 16, 17, 18, and 21.

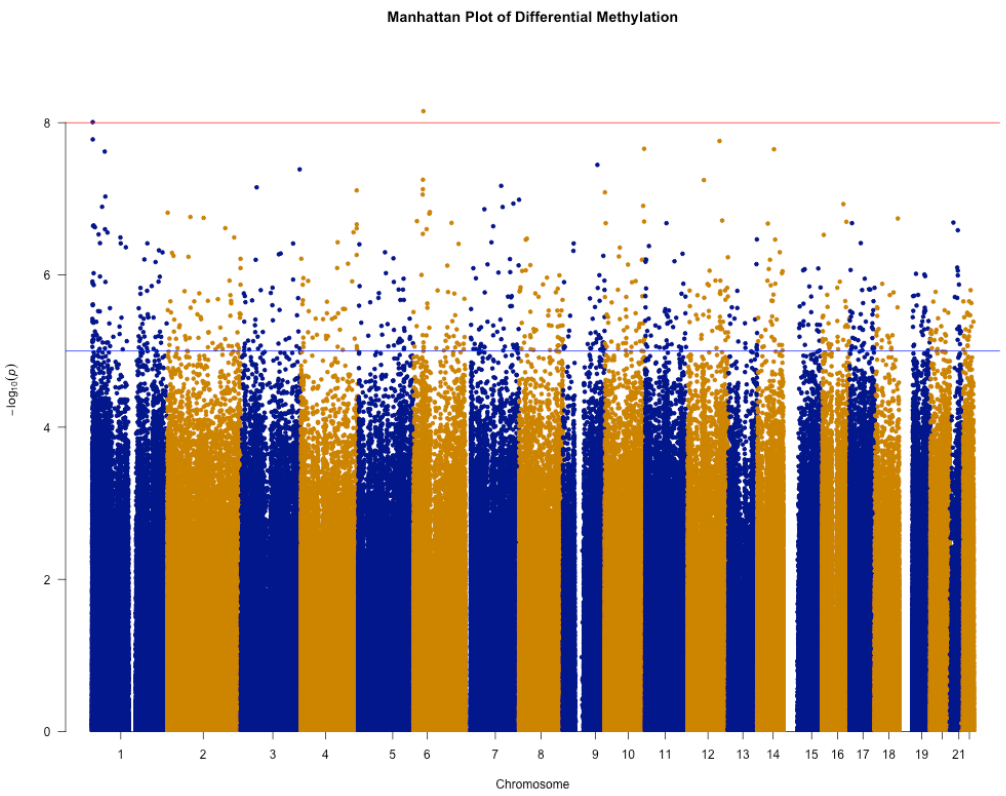

Figure 4.3. Manhattan plot depicting significant DMPs above the threshold value.

To isolate the most statistically robust and biologically relevant signals, a volcano plot was employed (Figure 4.4). The plot confirms a pronounced global imbalance: a significantly greater number of sites were hypermethylated (red) in ASD cases compared to controls, while a smaller subset was hypomethylated (blue). This trend suggests a predominant shift towards increased DNA methylation in the ASD cohort.

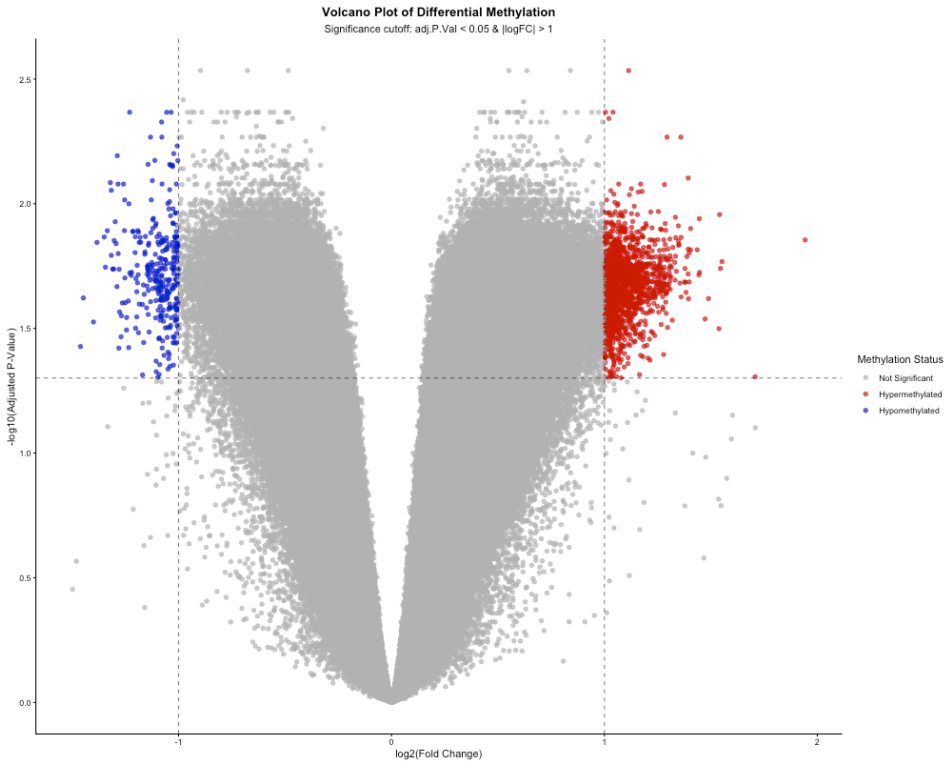

Figure 4.4. Volcano plot showing hypomethylated DMP sites in blue and hypermethylated ones in red.

Furthermore, the genomic context of these DMPs was investigated. Figure 4.5 illustrates their distribution relative to CpG islands. Notably, the hypermethylated DMPs showed a distinct profile: a majority (57.1%) were located within CpG island shores, while a near-equal split was observed for hypomethylated DMPs between shores and open sea regions. This indicates that ASD-associated hypermethylation is particularly enriched in regulatory regions flanking CpG islands.

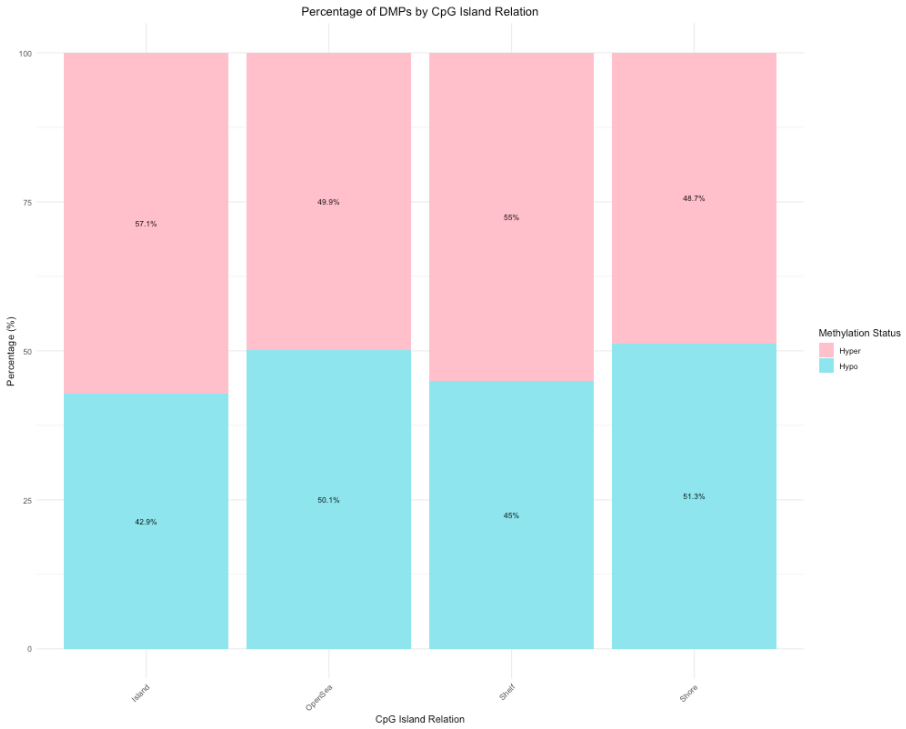

Figure 4.5. Percentage of DMPs hypermethylated and hypomethylated by CpG Island Relation.

Following the identification of individual CpG sites, the analysis was extended to identify broader, co-regulated genomic regions. A total of 15,560 Differentially Methylated Regions (DMRs) were identified across the genome, confirming that the epigenetic alterations in ASD are organized at a regional scale rather than being isolated events. These DMRs were subsequently annotated to determine their genomic context and potential functional impact.

The DMRs exhibited a clear imbalance in their methylation status, mirroring the trend observed at the single-site level. A total of 7,329 regions were significantly hypermethylated in ASD cases compared to controls. Conversely, 8,231 regions were significantly hypomethylated. This distribution indicates that while both directions of

change are widespread, a slight predominance of hypomethylation exists at the regional level, which may reflect distinct mechanisms of epigenetic dysregulation, such as alterations in broad chromatin domains or enhancer regions.

The genomic distribution of these DMRs was not uniform. As illustrated in Figure 4.6, the proportion of hypermethylated versus hypomethylated DMRs varied considerably by chromosome. Notably, chromosomes such as 16 and 19 showed a strong bias towards hypermethylation, with hypermethylated DMRs constituting 62.7% and 58.1% of significant regions, respectively. In contrast, chromosomes like 12 and 17 were dominated by hypomethylated DMRs, which accounted for 58.6% and 58.1% of findings. This chromosome-specific patterning suggests that distinct epigenetic regulatory mechanisms may be perturbed on different chromosomes in ASD.

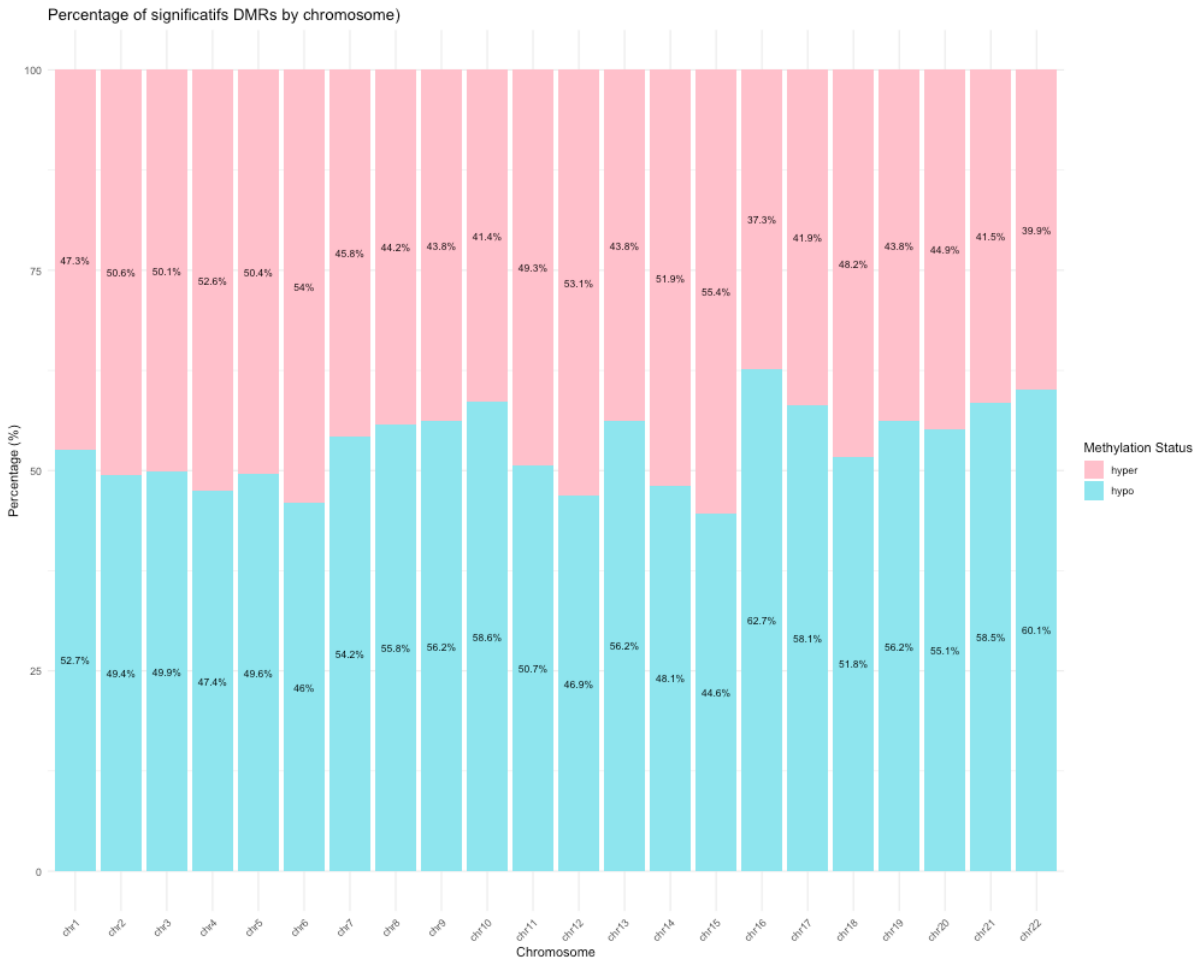

Figure 4.6. Percentage of DMRs hypermethylated and hypomethylated by chromosome.

4.2.2 *Functional annotation of hyper- and hypomethylated genes*

4.2.2.1 *Hypermethylated regions*

Functional annotation of hypermethylated DMRs revealed a highly significant enrichment for pathways related to innate immune activation. The most prominent GO terms included phagocytosis, Fc receptor–mediated signaling, type I interferon signaling, interferon-γ–mediated signaling, and Toll-like receptor 3 signaling. Additional categories

involved negative regulation of cytokine production, negative regulation of viral processes, and lymphocyte co-stimulation.

The consistent enrichment of antiviral and inflammatory pathways within hypermethylated loci suggests a potential epigenetic repression of innate immune responses, aligning with reports of attenuated interferon signaling and altered immune competence in subsets of individuals with ASD. This immune-related hypermethylation profile was robust and clearly distinguishable from the pattern observed in hypomethylated regions.

4.2.2.2 *Hypomethylated regions*

In contrast to the immune-dominated hypermethylation signature, hypomethylated DMRs were associated with pathways involved in cellular morphogenesis, differentiation, and cytoskeletal regulation. Enriched GO categories included protein trimerization, regulation of myotube differentiation, skeletal muscle contraction, nuclear migration, endocytic recycling, and regulation of mitochondrial membrane permeability. Notably, several terms implicated neurodevelopmental processes, including interneuron differentiation and the cerebellar-specific process “Purkinje cell–granule cell precursor signaling involved in regulation of granule cell precursor proliferation”. The presence of

this pathway suggests potential epigenetic involvement of cerebellar developmental mechanisms, a region increasingly recognized in ASD neuropathology.

Overall, hypomethylation appeared to preferentially affect genes involved in developmental patterning, cellular maturation, and intracellular transport, rather than immune regulation.

4.2.2.3 *Hypermethylated regions mapping to SFARI genes*

When restricting the analysis to hypermethylated DMRs associated with genes listed in the SFARI database, the enrichment profile diverged markedly from that of the full hypermethylation set. Immune-related categories were no longer among the top terms. Instead, enriched pathways involved vesicular trafficking and chromatin regulation, including uropod organization, plasma membrane to endosome transport, retrograde transport to the Golgi apparatus, covalent chromatin modification, and chromatin organization.

These findings reflect the functional composition of ASD risk genes, many of which encode regulators of synaptic protein trafficking and epigenetic remodeling (*i.e.*, CHD8, ARID1B, DNMT3A). Thus, SFARI-mapped hypermethylation appears to impact intracellular transport and transcriptional regulatory mechanisms, rather than innate immunity.

4.2.2.4 *Hypomethylated regions mapping to SFARI genes*

The subset of hypomethylated DMRs overlapping SFARI genes exhibited a strong and coherent enrichment for synaptic and neuronal signaling pathways, representing the most ASD-specific profile among all analyses performed. Highly significant GO terms included neuron-to-neuron synaptic transmission, trans-synaptic signaling, chemical synaptic transmission, and positive regulation of synaptic transmission. Additional enrichment for calcium ion transport, membrane depolarization, protein complex assembly, and chromatin modification underscores the involvement of genes governing synaptic structure, excitability, and transcriptional control.

These results indicate that hypomethylation preferentially affects genes central to synaptic function, neuronal communication, and neurodevelopmental regulation, consistent with the established roles of high-confidence ASD risk genes.

4.3 *Strenghts and Limitations*

The present methylation analysis integrates genome-wide DMR profiling with functional annotation using GREAT, enabling the identification of biological processes potentially influenced by epigenetic variation. A major strength of this approach is the ability to capture distal regulatory effects through GREAT's gene–region association model, and to

compare global versus ASD-specific (SFARI-restricted) functional signatures. This two-level framework increases interpretability by distinguishing general epigenomic signals from pathways specifically enriched among ASD risk genes.

However, some limitations must be acknowledged. GREAT relies on predicted regulatory domains rather than experimentally defined chromatin interactions, which may lead to imperfect gene assignment, particularly in gene-dense regions. Enrichment analyses are also inherently dependent on the completeness of available ontologies and may produce broad or overlapping categories. Finally, methylation data were derived from peripheral blood, which may not fully reflect brain-specific epigenetic patterns, although peripheral signatures can still provide relevant insight into systemic or developmentally regulated pathways.

5. Study III - Peripheral Biomarkers: Inflammation, Neurotrophic Factors, and Metabolic Pathways

5.1 *Materials and Methods for study III*

5.1.1 *Study Cohort for study III*

Patients were recruited at the Unit of Child Neurology and Psychiatry at the University Policlinic Hospital in Messina and were prospectively enrolled in the research program. The population has been selected according to the following inclusion criteria: (1) age ≥ 18 months; (2) individuals with confirmed diagnosis of ASD or with high risk of developing ASD; (3) naive to pharmaceutical therapy. Patients were screened for non-syndromic autism using echocardiogram and abdominal ultrasound, audiometry, urinary amino acids, and organic acids. Patients with dysmorphic features were excluded even in the absence of detectable cytogenetic alterations. Other exclusion criteria were an age > 6 years and the use of pharmacological treatment. Informed written consent to blood sampling and anamnestic data collection was obtained from parents of all recruited individuals.

5.1.2 *Clinical and neuropsychological evaluation*

Medical history was collected considering pre-, peri-, and postnatal variables for all patients. In particular, the following variables have been considered: family history of

ASD and other neurodevelopmental disturbances (including attention deficit/hyperactivity disorder (ADHD), intellectual developmental disorder, global developmental delay, language disorders), complicated pregnancy, preterm birth, APGAR score at the first and fifth minute of life, birthweight, cranial circumference at birth, impaired sucking and swallowing, gastroesophageal reflux, developmental milestones, age at onset of ASD symptoms, developmental regression, altered sleep–wake cycle, food selectivity, gastrointestinal problems, vitamin supplementation, rehabilitative intervention, peer group integration, screen use. Other variables were recorded during clinical evaluation, including atypical sensory processing (oral, visual, auditory, olfactory, tactile, vestibular), behavioural inflexibility, reliance on a transitional object, emotional dysregulation, stereotypies, hyperactivity, imitation skills, joint attention, pragmatic object exchange, response to name, and hypotonia.

Neuropsychological assessment included a developmental evaluation with the validated Italian translations of Griffiths Mental Development Scales Extended Revised (GMDS-ER), an autistic symptoms evaluation with the Autism Diagnostic Observation Schedule, Second Edition (ADOS-2), and an adaptive assessment with the Vineland Adaptive Behavior Scale-II (VABS-II).

5.1.3 *Biomarker analysis*

5.1.3.1 *Sample Collection*

Whole blood samples were collected and aliquoted into 300 µL fractions for the quantification of vitamin B2 and vitamin B6 levels.

Serum samples were centrifuged at 3,600 rpm for 5 minutes and rapidly stored at freezing temperature. These samples were subsequently used for the measurement of inflammatory cytokines and vitamin C.

5.1.3.2 *Cytokine Quantification by ELISA*

Quantitative determination of the cytokines under investigation was performed using an enzyme-linked immunosorbent assay (ELISA). In particular, a direct, non-competitive sandwich ELISA technique was employed, using commercial kits supplied by antibodies.com (Stockholm, Sweden).

Each cytokine was analyzed using a specific kit from the same manufacturer, differing only in reagent composition, as the experimental protocol was identical for all analytes.

The inflammatory cytokines analyzed were: Human Interleukin-1 alpha (IL-1α), Human Interleukin-1 beta (IL-1β), Human Interleukin-6 (IL-6), Human Interleukin-2 (IL-2), Interferon-gamma (IFN-γ).

5.1.3.3 *Principle of the Method*

The principle of the technique is based on the specific binding between an antibody and an antigen. An antigen is a molecule that can be recognized by the immune system, specifically by antibodies. In this assay, the antigens correspond to the cytokines to be detected, which are present in patient serum samples, while the antibodies are provided by the commercial kits.

The kit includes a 96-well microplate pre-coated with cytokine-specific immobilized antibodies. After addition to the wells, standards and samples bind to the capture antibodies during incubation. Subsequent washing steps allow removal of unbound material.

A biotinylated detection antibody specific for the cytokine of interest is then added, followed by additional washing steps to remove unbound antibody. Streptavidin–peroxidase conjugate (SABC) is subsequently added to each well and incubated. After further washing, tetramethylbenzidine (TMB) substrate is added. At this stage, the wells develop a blue color whose intensity is proportional to the concentration of cytokines present.

After a predefined incubation time, an acidic stop solution is added, resulting in a color change from blue to yellow. Absorbance is then measured at 450 nm using a spectrophotometer (Figure 5.1).

Figure 5.1. Main steps of the sandwich enzyme-linked immunosorbent assay (ELISA)

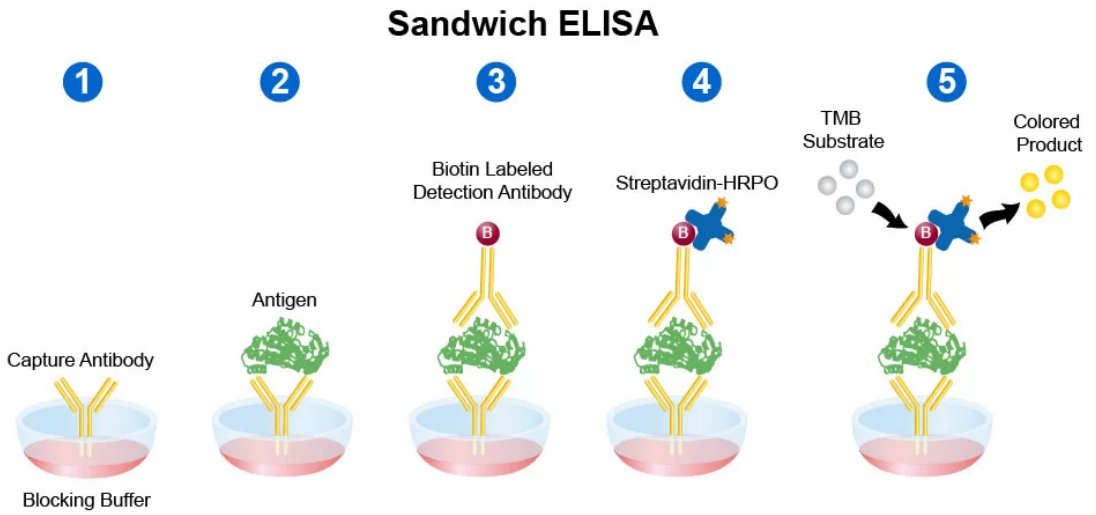

5.1.3.4 *Preparation of Reagents and Standards*

The wash buffer used for plate washing was prepared by diluting the 25× Wash Buffer concentrate provided in the antibodies.com kit with distilled water, according to the manufacturer's instructions (30 mL concentrate in 720 mL distilled water, final volume 750 mL).

Standards were prepared using the Sample Dilution Buffer supplied with the kit and lyophilized standard vials. Lyophilized standards were reconstituted with 1 mL of Sample Dilution Buffer to obtain the stock solution (Standard 0), which was mixed thoroughly and incubated at room temperature for 10 minutes. Serial dilutions were prepared from Standard 0 to Standard 6 (1:2 to 1:64) using Sample Dilution Buffer, while a blank sample containing only dilution buffer was included.

The total volume of biotinylated detection antibody was calculated based on a required volume of 100 µL per well, with an additional excess of 200 µL. The antibody was diluted 1:100 using the antibody dilution buffer provided in the kit.

Similarly, the total volume of Streptavidin–Peroxidase conjugate (SABC) was calculated based on 100 µL per well, with an additional excess of 200 µL, and diluted 1:100 according to the manufacturer's instructions.

5.1.3.5 *ELISA Protocol (antibodies.com Kit)*

Standards and serum samples diluted 1:2 with Sample Dilution Buffer were added to the wells (100 µL per well) and incubated at 37 °C for 90 minutes. After incubation, wells were washed twice using a plate washer. A biotinylated antibody specific for the cytokine of interest was then added (100 µL per well), followed by incubation at 37 °C for 60 minutes and three washing steps.

Subsequently, Streptavidin–Peroxidase conjugate (100 µL per well) was added and incubated at 37 °C for 60 minutes. After five washing steps, tetramethylbenzidine (TMB) substrate (90 µL per well) was added under light-protected conditions and incubated for 15 minutes at 37 °C. The reaction was stopped by the addition of acidic stop solution (50 µL per well), and absorbance was measured at 450 nm using a microplate reader.

5.1.3.6 *Vitamin B2 Quantification by HPLC*

Due to the photosensitivity of riboflavins, whole blood samples were protected from light by transferring 200 µL aliquots into dark tubes. Calibrators and controls were processed in parallel. Samples were treated with cold precipitation reagent P, vortexed, stabilized with reagent S, and centrifuged for 5 minutes at 10,000 rpm. The resulting supernatants were transferred into glass vials and analyzed by HPLC.

5.1.3.7 *Vitamin B6 Quantification by HPLC*

Vitamin B6 quantification was performed on whole blood samples protected from light by transferring 200 µL aliquots into dark tubes. After the addition of cold precipitation reagent P and vortexing, samples were centrifuged for 5 minutes at 10,000 rpm. Supernatants were subsequently transferred into glass vials and analyzed by HPLC.

5.1.3.8 *Vitamin C Quantification by HPLC*

For vitamin C analysis, 100 µL of serum samples, calibrators, and controls were transferred into 0.6 mL tubes and mixed with 100 µL of precipitation reagent P containing the internal standard. After vortexing, samples were incubated at 4 °C for 10 minutes and centrifuged at 10,000 × g for 10 minutes. The supernatants were then transferred into glass vials for HPLC analysis.

5.1.3.9 *Determination of Circulating Vitamin B9 Levels by ECLIA (Roche)*

Serum vitamin B9 (folate) levels were determined on serum samples using an electrochemiluminescence immunoassay (ECLIA). The assay is based on a competitive binding principle, in which folate present in the patient sample competes with a tracer-labeled folate analog for binding to a specific anti-folate antibody.

or the analytical procedure, 20 µL of non-hemolyzed serum were incubated with 300 µL of dithiothreitol-containing denaturation solution to induce protein denaturation and release protein-bound folate. The mixture was incubated at room temperature for 10 minutes.

Subsequently, 80 µL of reagent R1 were added, followed by incubation at room temperature for 9 minutes. Thereafter, 80 µL of reagent R2 were added and incubated for an additional 9 minutes at room temperature.

After these incubation steps, 20 µL of streptavidin-coated magnetic microparticles were added to the reaction mixture. The resulting immune complexes were magnetically captured onto the electrode surface by application of a magnetic field. Unbound material was removed by a washing step.

Electrochemiluminescence was then measured, and the emitted signal was directly proportional to the concentration of vitamin B9 present in the sample.

5.1.3.10 *Determination of Circulating Vitamin B12 Levels by ECLIA (Roche)*

Serum vitamin B12 levels were determined on serum samples using an electrochemiluminescence immunoassay (ECLIA). Prior to analysis, samples were pretreated to release vitamin B12 from protein binding.

The assay is based on a competitive binding principle, in which free vitamin B12 present in the sample competes with a ruthenium-labeled vitamin B12 for binding to intrinsic factor. The resulting immune complex is subsequently captured on streptavidin-coated microparticles and detected by electrochemiluminescence.

For the analytical procedure, 9 µL of serum or plasma were used. Samples underwent a pretreatment step to release protein-bound vitamin B12 by the addition of 30 µL of pretreatment reagents PT1 (dithiothreitol, DTT) and PT2 (sodium hydroxide and cyanide). The mixture was incubated at room temperature (37 °C) for 9 minutes.

Subsequently, 80 µL of reagent R1, consisting of ruthenium-labeled intrinsic factor, were added to initiate the competitive binding reaction. The mixture was incubated for 9 minutes.

In a second incubation step, 40 µL of streptavidin-coated microparticles (M) and 60 µL of biotinylated vitamin B12 (R2) were added to allow formation of the streptavidin–biotin immune complex. The reaction mixture was incubated for an additional 9 minutes.

Following incubation, the reaction mixture was transferred to the measuring cell, where magnetic capture of the immune complexes occurred. Unbound particles were removed by washing, and signal detection was performed by electrochemiluminescence measurement.

5.1.4 *Statistical analysis*

Categorical variables were expressed as absolute and percentage frequencies, whereas continuous variables were summarized as mean and standard deviation (SD).

Biochemical parameters provided with clinical reference ranges were dichotomized into “within range” and “out of range” according to age-adjusted lower or upper reference limits, as appropriate. Correlations between continuous variables were assessed using Spearman’s rank correlation coefficient.

Group comparisons according to ASD severity were performed using one-way ANOVA for continuous variables. For categorical variables, comparisons across the four severity groups were carried out using the chi-square test, or Fisher’s exact test when expected cell counts were <5.

The significance threshold was set at $\alpha = 0.050$ (two-tailed).

All statistical analyses were performed using SPSS software version 31.0 (IBM SPSS Statistics, Chicago, IL, USA).

5.2 *Results*

5.2.1 *Characterization of the study population*

Forty-nine individuals were enrolled in this study, 41 males (83,7%) and 8 females (16,3%). The mean age of the cohort at evaluation was 43,24 ± 9,13 months. Table 5.1 summarizes the anamnestic categorial features of the study cohort, reported as frequencies and percentages, while table 5.2 includes the anamnestic continuous variables, expressed as mean value ± SD.

Family history was frequently positive for neurodevelopmental and neuropsychiatric conditions, including ASD in 24.5% of the sample, language disorders in 20.4%, and other neuropsychiatric disorders in 44.9% of cases. Complicated pregnancy was reported in 40.8% of children, and 12.2% were born preterm. Developmental regression was documented in 20.8% of the cohort. Almost half of the children presented food selectivity (44.9%), 18.4% had gastrointestinal problems, and 28.6% showed an altered sleep–wake cycle, with insomnia and night awakenings reported in 8.2% and 20.4% of cases, respectively. All participants (100%) were engaged in rehabilitative intervention, with approximately half receiving standard rehabilitative treatment (46.9%) and just over half receiving behavioural treatment (53.1%). Peer group integration was present in 54.2% of children, while regular screen use was reported in 19%.

Perinatal and early developmental milestones were overall within the broad range expected for the paediatric population, although with considerable inter-individual variability. Mean birthweight was 3099.8 ± 476.07 g and mean cranial circumference at birth was 34.02 ± 1.99 cm. Apgar scores were generally high (8.88 ± 0.78 at 1 minute and 9.76 ± 0.43 at 5 minutes). Head control was attained at 3.21 ± 0.52 months, independent sitting at 6.42 ± 1.60 months, and independent walking at 14.50 ± 3.24 months. As expected, early communicative milestones showed wider dispersion: babbling emerged at a mean age of 8.68 ± 4.60 months, first single words at 16.95 ± 9.08 months, and pointing at 27.25 ± 10.90 months. The onset of ASD symptoms was estimated at 17.42 ± 6.61 months.

Table 5.1. Anamnestic categorial features of the study cohort

Feature	**Frequency (%)**
Family history of ASD	12 (24,5%)
Family history of ADHD	3 (6,1%)
Family history of IDD/DD	5 (10,2%)
Family history of language disorders	10 (20,4%)
Family history of other neuropsychiatric disorders	22 (44,9%)
Complicated pregnancy	20 (40,8%)
Preterm birth	6 (12,2%)
Impaired sucking [a]	2 (4,3%)
Impaired swallowing [a]	0 (0%)
Gastroesophageal reflux [a]	3 (6,5%)
Developmental regression [b]	10 (20,8%)
Food selectivity	22 (44,9%)

Gastrointestinal problems	9 (18,4%)
Altered sleep–wake cycle *Insomnia* *Night awakenings*	14 (28,6%) 4 (8,2%) 10 (20,4%)
Vitamin supplementation	3 (8,2%)
Rehabilitative intervention *Standard rehabilitative treatment* *Behavioural treatment*	49 (100%) 23 (46,9%) 26 (53,1%)
Peer group integration [b]	26 (54,2%)
Screen use [c]	8 (19%)

Legend: [a] n=46; [b] n=48; [c] n=42; ADHD = attention deficit/hyperactivity disorder; ASD = autism spectrum disorder; DD = developmental delay; IDD = intellectual developmental disorder

Table 5.2. Anamnestic continuous variables of the study cohort

Feature	**Mean value ± SD**
Birthweight [a]	3099,8 ± 476,07 g
Cranial circumference at birth [b]	34,02 ± 1,99 cm
Apgar score at 1' [c]	8,88 ± 0,78
Apgar score at 5' [c]	9,76 ± 0,43
Head control attained [d]	3,21 ± 0,52 mo
Sitting attained [a]	6,42 ± 1,6 mo
Independent walking attained [e]	14,5 ± 3,24 mo
Babbling attained (n=41)	8,68 ± 4,6 mo
Single words attained [b]	16,95 ± 9,08 mo
Pointing attained [f]	27,25 ± 10,9 mo
Age at onset of ASD symptoms [a]	17,42 ± 6,61 mo

Legend: [a] n=45; [b] n=20; [c] n=25; [d] n=42; [e] n=48; [f] n=16; mo= months; SD = standard deviation

All children underwent a standardized clinical and neurological evaluation. As detailed in Table 5.3, atypical sensory processing was highly prevalent, particularly in the visual (73.5%), vestibular (49%), tactile (38%), auditory (38%), and oral (38%) domains, whereas

olfactory alterations were rare (4.1%). Behavioural inflexibility was present in 46.9% of cases, and stereotypies were observed in 77.6% of the cohort. Emotional dysregulation affected 69.4% of children (49% mild and 20.4% moderate/severe), and hyperactivity was reported in 59.2%. Imitation skills were consistently present in 77.6%, although 32.7% showed only partial abilities. Joint attention was impaired in more than half of the children assessed (present in 45.7%), and pragmatic object exchange and response to name were frequently altered. Hypotonia was documented in 32.6% of the evaluated children.

Table 5.3. Clinical features of the study cohort

Feature	**Frequency (%)**
Atypical oral sensory processing	19 (38%)
Atypical visual sensory processing	36 (73,5%)
Atypical auditory sensory processing	19 (38%)
Atypical olfactory sensory processing	2 (4,1%)
Atypical tactile sensory processing	19 (38%)
Atypical vestibular sensory processing	24 (49%)
Auditory hypersensitivity	15 (30,6%)
Behavioural inflexibility	23 (46,9%)
Reliance on a transitional object	7 (14,3%)
Emotional dysregulation *Mild* *Moderate/severe*	34 (69,4%) 24 (49%) 10 (20,4%)
Stereotypies	38 (77,6%)
Hyperactivity	29 (59,2%)
Imitation skills	38 (77,6%)

Present/Consistent	22 (44,9%)
Partial	16 (32,7%)
Joint attention [a]	16 (45,7%)
Pragmatic object exchange [b]	23 (62,1%)
Complete	15 (40,5%)
Partial	8 (21,6%)
Response to name	19 (38,8%)
Hypotonia [c]	15 (32,6%)

Legend: [a] n=35; [b] n=37; [c] n=46

Neuropsychological assessment was performed at a mean age of 34.49 ± 9 months. Developmental evaluation with the GMDS-ER was available for all participants, whereas the ADOS-2 was administered to 44 children (7 assessed with the Toddler Module and 37 with Module 1), and the VABS-II was completed in 21 cases. As shown in Table 5.4, the mean General Development Quotient was 59.12 ± 15.86, with lower scores in the Hearing and Language domain (45.23 ± 19.16) compared to the Locomotor (68.97 ± 16.65), Personal–Social (56.03 ± 17.28), Eye–Hand Coordination (61.72 ± 18.56), and Performance (62.61 ± 19.30) subscales. Mean ADOS-2 total score was 14.55 ± 7, with a Social Affect score of 11.84 ± 6 and an RRB score of 2.80 ± 2.93. VABS-II Adaptive Behavior Composite scores were low overall (62.33 ± 15.66), with similar reductions in Communication, Daily Living Skills, and Socialization domains.

Table 5.4. Neuropsychological assessment results of the study cohort

	Assessment	Mean value ± SD
GMDS-ER	General development Quotient	59,12 ± 15,86
	Locomotor Quotient	68,97 ± 16,65
	Personal-Social Quotient	56,03 ± 17,28
	Hearing and language Quotient	45,23 ± 19,16
	Eye-hand coordination Quotient	61,72 ± 18,56
	Performance Quotient	62,61 ± 19,3
ADOS-2	Total Score	14,55 ± 7
	SA score	11,84 ± 6
	RRB score	2,8 ± 2,93
VABS-II	Adaptive Behavior Composite	62,33 ± 15,66
	Communication	55,24 ± 22,03
	Daily Living Skills	66,9 ± 20,88
	Socialization	68,52 ± 12,95

Legend: ADOS-2=Autism Diagnostic Observation Schedule, Second Edition; GMDS-ER=Griffiths Mental Development Scales Extended Revised; RRB=Restricted and Repetitive Behaviors; SA=Social Affect; SD=standard deviation; VABS-II=Vineland Adaptive Behavior Scale-II

Severity stratification was performed on the basis of clinical presentation and standardized neuropsychological scores. Children were categorized into four groups: autistic traits or at high-risk of ASD (n=10), mild ASD (n=20), moderate (n=12), and severe ASD (n=7).

5.2.2 *Biological markers*

A comprehensive panel of biochemical markers was obtained in the same cohort, with sample size varying slightly across parameters. The analytes included metabolic markers

(homocysteine, folic acid, vitamin B12, vitamin B2, vitamin B6, vitamin C, vitamin D), immunoglobulins (IgA, IgG, IgM), inflammatory markers (C-reactive protein, erythrocyte sedimentation rate, Anti-Streptolysin O titer), and, in a subset of children, cytokines and growth factors (IL-1α, IL-1β, IL-2, IL-6, IFN-γ, and NGF). Of the total sample, three children were undergoing vitamin supplementation at the time of blood collection. As supplementation can modify circulating levels independently of endogenous metabolic status, these participants were excluded from the descriptive statistics and correlation analyses involving vitamin markers. Mean values, standard deviations, and the proportion of children falling outside age-adjusted reference ranges are reported in Table 5.5.

Homocysteine levels (n = 45) showed a mean of 15.75 ± 47.95 µmol/L, with 75.6% of children presenting values above the reference range. Folic acid (n = 46) had a mean concentration of 7.21 ± 4.23 ng/mL, with 19% of values under the range. Vitamin B12 (n = 47) had a mean of 753.36 ± 279.32 pg/mL, with 18.6% out-of-range measurements. For the other B-complex vitamins, mean levels were 278.25 ± 90.60 µg/L for vitamin B2 (16.3% out of range) and 33.21 ± 18.88 µg/L for vitamin B6 (65.1% out of range). Vitamin C levels averaged 9.48 ± 13.99 mg/L (58.1% out of range), whereas vitamin D showed a mean value of 27.74 ± 11.37 µg/L, with 22.5% of children under recommended limits.

Immunoglobulin levels (n = 47) were within paediatric ranges in most children, with mean values of 87.94 ± 35.75 mg/dL for IgA, 914.57 ± 174.27 mg/dL for IgG, and 110.27 ± 53.48 mg/dL for IgM. Inflammatory markers showed low median systemic inflammation: CRP had a mean of 0.43 ± 1.47 mg/dL, ESR (n = 44) averaged 10.44 ± 10.40 mm/h, and ASO titers were 105.9 ± 214.97 IU/mL. Among cytokines and growth factors (measured in 19–25 children depending on the analyte), mean concentrations were 207.97 ± 182.07 pg/mL for IL-1α, 321.50 ± 280.07 pg/mL for IL-1β, 699.34 ± 663.38 pg/mL for IL-2, 7.50 ± 3.63 pg/mL for IL-6, 589.69 ± 725.60 pg/mL for IFN-γ, and 258.37 ± 395.25 pg/mL for NGF.

One-way ANOVA across the four ASD severity groups (autistic traits/high risk, mild, moderate, severe) did not reveal significant differences in any of the biochemical markers, including metabolic, inflammatory, and immunological parameters (all $p > 0.05$). This suggests that, at the group level, biochemical profiles were relatively homogeneous across severity clusters, despite the clinical and developmental heterogeneity described above.

Table 5.5. Peripheral Biochemical, Immune, and Neuroinflammatory Markers: Mean Values and Percentage Out of Reference Range

Biological markers	**Mean value ± SD**	**% out of range**
Homocysteine [a]	15,75 ± 47,95 umol/l	75,6%
Folic acid [b]	7,21 ± 4,23 ng/ml	19%
Vitamin B12 [c]	753,36 ± 279,32 pg/ml	18,6%
Vitamin B2 [a]	278,25 ± 90,6 ug/l	16,3%

Vitamin B6 [a]	33,21 ± 18,88 ug/l	65,1%
Vitamin C [a]	9,48 ± 13,99 mg/l	58,1%
Vitamin D [d]	27,74 ± 11,37 ug/l	22,5%
IgA [c]	87,94 ± 35,75 mg/dl	0%
IgG [c]	914,57 ± 174,27 mg/dl	0%
IgM [c]	110,27 ± 53,48 mg/dl	17%
CRP	0,43 ± 1,47 mg/dl	87,8%
ESR [d]	10,44 ± 10,4	79,5%
ASO titer	105,9 ± 214,97 IU/ml	85,7%
IL-1α [e]	207,97 ± 182,07 pg/ml	8%
IL-1β [e]	321,5 ± 280,07 pg/ml	8%
IL-2 [e]	699,34 ± 663,38 pg/ml	0%
IL-6 [f]	7,5 ± 3,63 pg/ml	52,6%
IFN-γ [e]	589,69 ± 725,6 pg/ml	0%
NGF [g]	258,37 ± 395,25 pg/ml	25%

Legend: [a] n=45; [b] n=46; [c] n=47; [d] n=44; [e] n=25; [f] n=19; [g] n=16; ASO=Anti-Streptolysin O; CRP=C-reactive protein; ESR=Erythrocyte Sedimentation Rate; IL=interleukin; IFN=interferon; SD = standard deviation

5.2.3 *Biochemical–Endophenotypic Correlations*

Spearman correlation analyses identified several significant associations between biochemical parameters and developmental functioning, ASD symptom severity, and clinical endophenotypes. Although these correlations do not imply causality, they highlight patterns that may be relevant for characterising biological subgroups within the cohort.

Regarding developmental outcomes (GMDS-ER), CRP showed consistent positive correlations with the global developmental quotient and with the motor, personal–social,

language, eye–hand coordination, and performance domains. This pattern suggests that, in this sample, higher CRP values tended to co-occur with relatively higher developmental scores, an unexpected direction but one that may reflect underlying heterogeneity in systemic inflammation across subgroups. Vitamin C also correlated positively with motor and eye–hand coordination scores, indicating that higher circulating vitamin C levels were associated with more favourable performance in these domains. In contrast, homocysteine showed negative associations with language and performance, consistent with its general role as a metabolic stress marker. Folate displayed positive correlations with eye–hand coordination and performance, while IgM correlated positively with motor and personal–social functioning. ESR also showed positive associations with coordination and performance. Vitamin D, however, correlated negatively with personal–social functioning and performance, indicating an inverse relationship in these two areas.

ASD symptom severity showed a clearer and more homogeneous pattern: both ADOS total scores and specific subdomains were inversely correlated with all Griffiths developmental quotients, with moderate-to-strong coefficients. This indicates that, within the cohort, greater ASD symptom burden was systematically associated with lower developmental functioning across domains, reflecting the expected clinical gradient.

Associations with sensory and behavioural endophenotypes were more domain-specific. Oral sensory seeking correlated positively with object transition difficulties and hypotonia, suggesting that children with heightened oral sensory behaviours tended to present more challenges in motor–regulatory domains. Visual sensory sensitivities were linked to rigidity, joint attention difficulties, and reduced response to name, pointing toward a cluster in which visual reactivity co-occurs with social–adaptive challenges. Auditory sensory scores were associated with auditory hypersensitivity, as expected. Imitation abilities showed negative correlations with gesture use and stereotypies, while joint attention was positively associated with multiple behavioural measures, including rigidity, gesture use, and response to name, thus indicating that social-communicative endophenotypes were interrelated across multiple levels of observation.

Biochemical–endophenotype correlations were more selective. IgA correlated positively with tactile processing and with response to name, while IgM showed a positive association with visual sensory reactivity. CRP demonstrated several negative associations, including with oral sensory behaviours, rigidity, and stereotypies, suggesting that individual variability in low-grade inflammation might relate to behavioural organisation. ESR correlated positively with visual and tactile sensory reactivity. Folate was negatively associated with object transition difficulties, and vitamin C showed a negative correlation with tactile scores. Cytokines such as IL-1α, IL-1β, IL-2,

IFN-γ, and NGF exhibited isolated negative associations with specific developmental or behavioural measures, without forming a coherent or reproducible pattern across domains, likely reflecting the smaller sample size available for cytokine analyses.

Figure 5.1 summarizes the significant associations between biochemical markers and the developmental, sensory, and behavioral endophenotypes, illustrating the specific domains in which each marker showed meaningful correlations. Overall, these correlations delineate clusters of biochemical–behavioural associations that may help to identify subgroups with shared developmental and metabolic profiles.

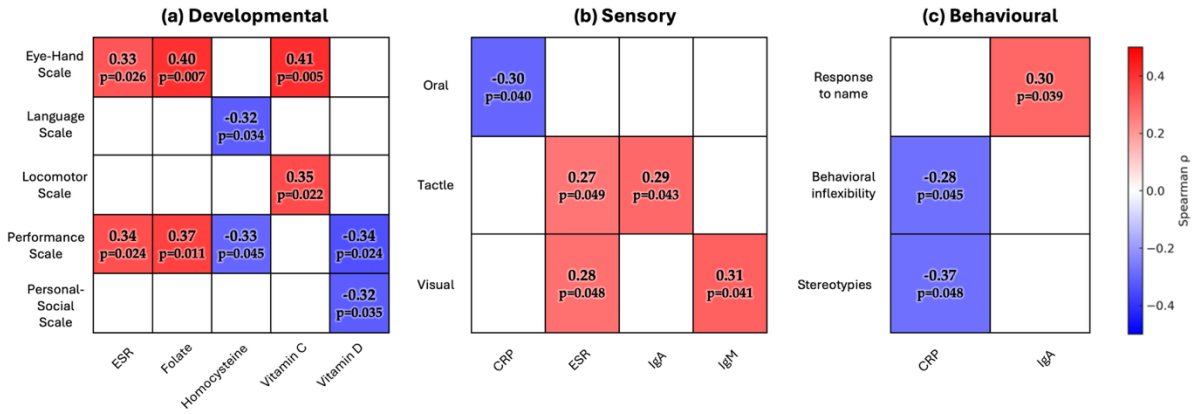

Figure 5.1. Heatmap of significant correlations between biochemical markers and developmental, sensory, and behavioral endophenotypes

Panels show Spearman's correlations between each biomarker and the corresponding set of clinical measures: (a) developmental outcomes, (b) sensory endophenotypes, and (c) behavioral features. Only correlations reaching statistical significance ($p < 0.05$) are displayed. Cell colors represent the direction and magnitude of the correlation (blue = negative; red = positive), with rho values and associated p-values shown inside each cell. A shared color scale is provided on the right.

As an exploratory analysis, categorical biochemical variables (within range vs. out of range) were examined to assess whether clinically abnormal values aligned with developmental, sensory, or behavioural features. A small number of significant associations emerged. Out-of-range vitamin C values were associated with greater tactile reactivity, and vitamin D deficiency was linked to increased auditory sensitivity. Reduced folate values correlated with lower motor and performance scores, whereas increased homocysteine levels showed a positive association with restricted and repetitive behaviours. No significant associations were observed for vitamin B12 and vitamin B2.

Out-of-range analyses were not performed for inflammatory markers or immunoglobulins because reference cut-offs in early childhood are highly age-dependent and less standardised than those available for metabolic and vitamin markers. To avoid misclassification and ensure more accurate interpretation, these parameters were analysed solely as continuous variables. These findings should be interpreted cautiously, as dichotomisation of biochemical variables reduces statistical power and may not fully capture physiological variability; however, they provide complementary information to the continuous-variable analyses.

5.3 Stenghts and Limitations

This study offers several strengths, including the comprehensive phenotypic characterization of a pharmacologically naïve cohort of young children with ASD or high likelihood of ASD, assessed through standardized neurodevelopmental tools and detailed clinical evaluation of sensory and behavioural endophenotypes. The broad biochemical panel, encompassing metabolic, inflammatory, immunological, and neurotrophic markers, enabled a multidimensional exploration of potential biological correlates.

At the same time, several limitations should be acknowledged. The sample size (particularly for cytokine and growth factor analyses) was relatively small, limiting statistical power and restricting the use of more advanced multivariate approaches. The cross-sectional design prevents any temporal or causal inference, and single time-point biochemical measures may not capture intra-individual variability. Finally, although sensory and behavioural features were systematically evaluated, their clinical nature may introduce measurement variability, and the inherent heterogeneity of ASD may have contributed to overlapping profiles across severity groups.

6. Study IV - Exploratory Analysis of MRI and EEG Biomarkers

6.1 Materials ad Methods

6.1.1 *Study design and participants for study IV*

This retrospective study included all pediatric patients with a confirmed diagnosis of ASD who had undergone both brain MRI and EEG as part of their diagnostic evaluation since the 01/01/2022 to the 31/03/2025 at the Unit of Child Neurology and Psychiatry at Polyclinic Hospital University in Messina (Italy). Clinical, neurophysiological, neuroimaging, and developmental data were extracted from electronic medical records. Exclusion criteria comprised: (1) syndromic or genetically determined neurodevelopmental disorders; (2) evidence of acquired brain injury, including hypoxic–ischemic, ischemic, or hemorrhagic lesions; (3) neurological conditions that could independently account for MRI or EEG abnormalities; and (4) incomplete clinical records.

6.1.2 *Neuroimaging and neurophysiological assessment*

Brain MRI examinations had been performed as part of routine clinical evaluation using standardized pediatric protocols. MRI reports were reviewed and categorized according to the presence of neurodevelopmental features commonly described in ASD, including variations in corpus callosum morphology, hippocampal developmental anomalies, white matter abnormalities (white matter dysgenesis or minor lesional patterns), and

other non-lesional findings. Each MRI feature was coded as present or absent, and an additional variable captured the presence of any neurodevelopmental MRI atypicality.

EEG recordings obtained during wakefulness and/or sleep were reviewed based on the original clinical reports. EEGs were categorized as normal, para-physiologic variants, or abnormal, with specific identification of epileptiform activity. A clinical diagnosis of epilepsy was recorded when present. EEG variables were analysed both categorically and in association with MRI features.

6.1.3 *Clinical and behavioural characterization*

Perinatal and neonatal information was extracted from clinical records and included: family history of neurodevelopmental disorders; type of pregnancy (singleton or twin); medically assisted reproduction; gestational age; birthweight; birth length; and head circumference. Additional variables included threatened miscarriage, maternal complications or treatments during pregnancy (tocolytics, thrombophilia, steroid use, psychotropic and antiepileptic medications), mode of delivery, prenatal infections, Apgar scores at 1 and 5 minutes, intrapartum fetal distress, neonatal intensive care admission, pathological neonatal jaundice, and neonatal sepsis or infections.

Developmental, cognitive, adaptive, and behavioural features were collected from diagnostic assessments and clinical documentation. Functional severity was indexed

using the clinician-rated level of required support. Additional clinical variables included language delay, aggressive behaviour, and gastrointestinal problems.

6.1.4 *Statistical analysis*

Descriptive statistics were used to summarize neuroimaging findings, neurophysiological patterns, and perinatal variables. Associations between categorical variables were tested using chi-square analyses. Ordinal logistic regression models (PLUM) were performed to evaluate whether MRI or EEG features predicted cognitive classification or level of required support. Independent variables included MRI categories, EEG abnormalities, epilepsy, and selected clinical or behavioural features. Statistical significance was set at $p < 0.05$.

6.2 Results

Clinical and perinatal data were retrospectively collected for children with ASD who underwent neuroimaging and neurophysiological assessments. The characteristics of the study cohort are summarized in Table 6.1 and Table 6.2, with categorical variables reported as frequencies and percentages and continuous variables expressed as mean ± SD respectively.

Table 6.1. Categorical demographic, perinatal, and clinical characteristics of the study cohort

Variable	**Frequency**
Sex (male)	73%
Family history of neurodevelopmental disorders	51%
Singleton pregnancy	90,8%
Medically assisted reproduction	5,5%
Threatened miscarriage [a]	31,9%
Tocolytic therapy during pregnancy [b]	12,1%
Maternal thrombophilia [c]	5%
Steroid therapy during pregnancy [d]	4,3%
Prenatal infections [d]	3,1%
Emergency caesarean section [e]	22%
Intrapartum fetal distress [a]	16,9%
NICU admission [e]	11,9%
Pathological neonatal jaundice [f]	7%
Neonatal sepsis or infections [e]	2,5%
Language delay [d]	87%
Nonverbal	32,5%
Aggressive behaviour	31,5%
ADHD	57,1%
DCD	21,3%
OCD	3,7%
Psychotic episode	2,5%
Tic disorder	2,5%
Food selectivity	39,8%
Sleep disorder	31,7%
Gastrointestinal problems	29,8%
Hypotonia	12,3%

Legend: [a] n=160; [b] n=157; [c] n=161; [d] n=162; [e] n=159; [f] n=158; ADHD = Attention Deficit/Hyperactivity Disorder; DCD = Developmental Coordination Disorder; OCD = Obsessive Compulsive Disorder

Table 6.2. Continuous demographic, perinatal, and clinical characteristics of the study cohort

Variable	**Mean ± SD**
Gestational age (weeks)	38,62 ± 2,17
Birth weight (g)	3109,62 ± 550,39
Birth length (cm)	49,03 ± 2,98
Head circumference (cm)	34,31 ± 2,57
Apgar score at 1 minute	7,99 ± 1,51
Apgar score at 5 minutes	9,18 ± 1,05
Age (years)	7,88 ± 3,84

6.2.1 *Characterization of neuroimaging alterations*

Brain MRI abnormalities were highly prevalent in the cohort. Overall, 76.1% of children showed at least one structural alteration on MRI, while only 23.9% had a completely normal scan. The most frequent findings involved the corpus callosum, with anomalies detected in 36.2% of individuals, predominantly affecting the body of the structure. Alterations of the hippocampal formation were also common (41.1%), and more than half of the sample (55.8%) presented other structural abnormalities across different brain regions. White matter anomalies were identified in a minority of children, with white matter dysgenesis patterns in 4.3% and lesional alterations in 14.8%.

No significant associations emerged between corpus callosum anomalies and cognitive level or level of support required, nor between hippocampal involvement and clinical severity categories. Likewise, MRI abnormalities of any type were not associated with cognitive classification levels. A marginal trend suggested that children with a

pathological MRI were more frequently classified in higher support categories, but the association did not reach statistical significance. Table 6.3 summarizes the frequencies of the neuroimaging findings.

Table 6.3. MRI findings of the study cohort

MRI feature	**Frequency**
Any MRI atypicality	76.1%
Corpus callosum abnormalities	36.2%
Hippocampal abnormalities	41.1%
White matter abnormalities	20.3%

6.2.2 *Neurophysiological findings*

Electroencephalographic recordings were available for most participants. EEG abnormalities were observed in 26.9% of children, while epileptiform activity was present in 24.5%. Clinical epilepsy was diagnosed in 19% of the cohort.

A significant association emerged between MRI abnormalities and EEG findings: children with a pathological MRI were more likely to exhibit EEG anomalies compared to those with normal scans. However, no association was detected between MRI alterations and the presence of clinical epilepsy. Similarly, corpus callosum abnormalities were not significantly related to either EEG category or epileptic activity. Table 6.4 summarizes the frequencies of the EEG findings.

Table 6.4. EEG findings in the study cohort

EEG feature	**Frequency**
Non-pathological EEG abnormalities	26.9%
Epileptiform activity	24.5%
Epilepsy	19.0%

6.2.3 *Associations with clinical and behavioural features*

The investigation of clinical features revealed no significant correlations between MRI anomalies and behavioural comorbidities such as ADHD or aggressive behaviours. Likewise, EEG anomalies did not predict the level of support required.

Ordinal regression models further confirmed that neuroimaging and neurophysiological biomarkers did not independently predict either cognitive classification or support level. Instead, clinical and functional characteristics, including aggressive behaviour, language delay, and gastrointestinal functional problems, emerged as more relevant predictors in models assessing support needs. The results of the ordinal regression analyses are summarized in Table 6.5.

Table 6.5. Ordinal logistic regression (PLUM) predicting level of required support

Predictor	**Estimate (β)**	**SE**	**Wald**	**p-value**	**95% CI**
Aggressive behavior	0.974	0.333	8.536	0.003	0.321–1.627
Gastrointestinal problems	0.911	0.340	7.177	0.007	0.244–1.577
Language delay	1.041	0.438	5.642	0.018	0.182–1.900

6.2.3 *Clinical correlates of functional outcome*

A set of perinatal and neonatal variables was examined to explore potential associations with the neurodevelopmental MRI features identified in the cohort, including hippocampal anomalies, white-matter developmental alterations, corpus callosum variations, and other atypical patterns commonly described in ASD. Among these variables, pathological neonatal jaundice emerged as the only factor significantly associated with specific MRI findings. Children with a history of pathological jaundice were substantially more likely to exhibit hippocampal abnormalities ($\chi^2 = 11.389$, $p = 0.001$), representing the strongest association detected in the perinatal domain. In contrast, jaundice showed no significant relationship with white matter anomalies, corpus callosum features, or other MRI categories (all $p > 0.05$). Although a trend toward higher white-matter anomalies was observed in children with jaundice, this association did not reach statistical significance. Significant univariate associations identified between perinatal factors, MRI findings, and EEG abnormalities are reported in Table 6.6. Other perinatal and neonatal factors (including prenatal infections, intrapartum fetal distress, neonatal sepsis or infections, and Apgar scores) did not show significant associations with any MRI feature. These findings indicate that, within this cohort, hippocampal maturation appears particularly sensitive to early-life bilirubin-related neurotoxicity, whereas most commonly reported perinatal conditions were not linked to

the neurodevelopmental MRI patterns typically observed in children with ASD. Importantly, no lesion-type MRI patterns (i.e., hypoxic–ischemic injury) were identified in association with any neonatal complication.

Table 6.6. Univariate associations between perinatal, neuroimaging, and neurophysiological variables

Domain	**Predictor**	**Outcome**	**p-value**
Perinatal	Pathological neonatal jaundice	Hippocampal abnormality	0.001
Perinatal	Pathological neonatal jaundice	Any MRI abnormality	0.017
Neuroimaging	Any MRI abnormalities	EEG abnormality	0.028

6.3 *Strengths and Limitations*

This study offers a broad and integrated view of neurodevelopmental MRI features and EEG patterns in a relatively large cohort of children with ASD, combining neuroimaging, neurophysiological, clinical, and perinatal information within a single analytical framework. The systematic categorization of MRI and EEG findings and the use of multivariable ordinal regression models strengthened the evaluation of potential contributors to functional outcomes.

Nevertheless, several limitations should be acknowledged. The retrospective design relied on clinical documentation, which may have limited the completeness and precision of some variables. MRI and EEG data were based on routine clinical reports

rather than standardized research protocols, reducing the granularity of certain findings. The exclusion of lesion-type MRI abnormalities ensured a more homogeneous sample but may restrict generalizability. Finally, although the cohort was adequate for descriptive analyses, less frequent perinatal factors may have been underpowered to reveal subtle associations.

7. Discussion

The findings of this thesis suggest that ASD should not be viewed as a single biological condition, but rather as a collection of partially overlapping neurobiological trajectories influenced by genetic, epigenetic, metabolic, immune, and neurodevelopmental factors. When examined collectively, the findings from the four complementary studies reveal patterns of coherence across biological domains, suggesting the presence of definable endophenotypic dimensions that could substantially refine our understanding of ASD heterogeneity. At the same time, the results underscore significant methodological and conceptual challenges that continue to limit the translation of biological signatures into clinically actionable subgroups.

The genetic findings of this study strongly support the idea that variation in antioxidant and detoxification pathways contributes to a biologically meaningful susceptibility axis in ASD. This aligns with an extensive body of evidence demonstrating increased oxidative

damage and impaired redox homeostasis in autistic individuals [27–29]. Among the most compelling associations is the GPx1 rs1800668 TT genotype, observed exclusively in ASD and consistent with longstanding evidence that glutathione-dependent antioxidant defenses are compromised in this condition [30,31].

The enrichment of the PON1 Q192R mutated genotype further supports a gene–environment interaction model, given PON1's key role in detoxifying organophosphates and preventing oxidative lipid damage. Prior studies have repeatedly linked PON1 variants to neurodevelopmental vulnerability [32,33], and broader epidemiological work underscores the contribution of toxic chemicals to ASD etiology [34].

The results concerning SOD2 A16V reflect the heterogeneous literature on SOD activity in ASD, where both increased and decreased activity have been reported [35]. Few studies have examined SOD gene variants directly, and available findings are inconsistent [36,37]. The present data suggest that SOD2 may modulate individual oxidative stress levels rather than act as a categorical risk factor, consistent with pathway-based vulnerability models [38].

The CAT –844C>T association represents novel evidence linking catalase polymorphisms to ASD. Although catalase activity findings in ASD have been mixed, even subtle reductions in hydrogen peroxide detoxification could sensitize the developing brain to

oxidative injury, particularly given its high metabolic demand and inherently low antioxidant reserves [39].

Detoxification-related variants also contributed to risk patterns. GSTT1 deletion, and particularly combined GSTM1/GSTT1 deletions, have been associated with increased vulnerability to toxicant-induced oxidative stress and poorer neurodevelopmental outcomes [40,41], a finding mirrored in this cohort.

Finally, the enrichment of impaired-metabolizer alleles in CYP2D6, CYP2C9, and UGT1A1 suggests that metabolic vulnerabilities may extend beyond risk to influence treatment outcomes. Poor metabolizer CYP2D6 alleles, for example, have been associated with altered risperidone pharmacokinetics and increased side effects in autistic children [42–44], while UGT1A1*6 variants have been linked to neonatal hyperbilirubinemia, a proposed perinatal ASD risk factor [45].

Taken together, these findings delineate a coherent redox–detoxification endophenotype, where genetic vulnerability to oxidative stress and xenobiotics converges with measurable biological alterations such as elevated AOPP and DNA damage [24,46]. Together, these observations indicate that oxidative stress may play a contributory role in shaping developmental trajectories in a subset of autistic individuals.

The epigenomic findings of this study support the view that ASD risk is influenced by dynamic gene–environment interactions acting during early neurodevelopment, rather

than by static genetic variation alone. In line with genome-wide and targeted epigenetic studies, the DNA methylation changes identified in our cohort preferentially involved regulatory regions of genes implicated in synaptic function, neuronal differentiation, immune signaling, and metabolic pathways, supporting the concept that epigenetic dysregulation represents a relevant molecular interface between inherited susceptibility and environmental exposures [47–49]. Large methylome-wide association studies have shown that ASD-associated methylation signatures can be detected not only in brain tissue but also in peripheral tissues such as cord blood and placenta, suggesting that epigenetic alterations may arise early in development and precede clinical manifestation [50,51]. The partial convergence between methylation patterns observed in neonatal tissues and those reported in post-mortem brain samples, particularly within pathways related to neuronal connectivity and microglial function, further supports the biological relevance of peripheral epigenetic findings [49,51].

Within this framework, our data revealed a clear dissociation between immune-related and neurodevelopmental pathways. Hypermethylated regions were predominantly enriched in innate immune signaling pathways, including interferon-mediated responses, Fc receptor signaling, and Toll-like receptor cascades. This pattern is consistent with an epigenetically downregulated immune profile rather than with overt immune activation, in agreement with reports suggesting that immune alterations in ASD

may reflect impaired immune responsiveness or altered immune maturation rather than chronic inflammation [50,51]. Comparable immune-related methylation signatures have been described in cord blood and placental tissues of children later diagnosed with ASD, indicating that such epigenetic modulation may be established prenatally and persist across development [50].

Conversely, hypomethylated regions in our study were enriched in genes involved in neuronal differentiation, cytoskeletal organization, synaptic signaling, mitochondrial membrane dynamics, and cerebellar development. This pattern closely mirrors findings from multiple EWAS and MWAS studies reporting preferential hypomethylation of neurodevelopmental and synaptic pathways in ASD, particularly in genes regulating neuronal connectivity and plasticity [48,49]. The directionality observed in our data is consistent with the interpretation that hypomethylation may reflect increased transcriptional permissiveness during critical periods of brain development, potentially contributing to atypical circuit formation.

Notably, when analyses were restricted to SFARI-annotated genes, both hyper- and hypomethylated regions converged on pathways involved in chromatin regulation, vesicular trafficking, and synaptic transmission. This convergence suggests that epigenetic alterations in ASD preferentially affect regulatory hubs with broad downstream effects rather than isolated loci, consistent with previous reports describing

epivariations and variably methylated regions enriched at developmentally relevant regulatory sites [48]. Such network-level effects may help explain how relatively modest methylation changes can be associated with substantial phenotypic variability.

The overall structure of our epigenomic findings further supports a gene–environment interaction model. Epigenetic marks are particularly sensitive to prenatal and early postnatal exposures, and the pathways identified in our study overlap with those reported in epigenetic investigations linking environmental risk factors (i.e., metabolic stress, immune perturbations, and xenobiotic exposure) to ASD-relevant methylation changes [50,52]. In this context, the immune-related hypermethylation observed may be interpreted as an adaptive or compensatory response to early environmental challenges rather than as a primary pathogenic mechanism.

An additional interpretative framework emerges from evidence indicating that epigenetic regulation during neurodevelopment is strongly influenced by metabolic state, redox balance, and B-vitamin availability, which can modulate DNA methylation and chromatin organization without necessarily producing pathway-specific epigenetic signatures [52,53]. In this light, the convergence between the epigenomic alterations observed in this study and the metabolic findings reported in other components of this thesis suggests that these biological layers may be functionally interconnected rather than independent.

Importantly, our findings are consistent with literature indicating that ASD-associated epigenetic signatures can be detected across multiple tissues while showing partial convergence with brain-derived data. The overlap between pathways identified in peripheral tissues and those reported in post-mortem brain studies (particularly involving synaptic, immune, and chromatin-related genes) supports the biological relevance of our peripheral epigenomic results, while also highlighting inherent limitations related to tissue specificity [49,51]. As reported in previous studies, effect sizes of methylation changes were modest, and the cross-sectional design limits inference on temporal dynamics, indicating that individual CpG sites are unlikely to function as standalone biomarkers [49].

Taken together, these findings support the existence of an epigenetic endophenotype characterized by coordinated dysregulation of immune and neurodevelopmental pathways, likely established early in development and modulated by environmental and metabolic factors. Rather than defining a uniform ASD signature, this epigenetic profile may contribute to interindividual variability and interact with genetic and biochemical vulnerability axes identified elsewhere in this thesis, reinforcing the value of integrated stratification models in ASD research.

The clinical–biochemical analyses performed in this cohort indicate that peripheral metabolic and immune markers are selectively associated with specific developmental

and behavioural domains rather than with global ASD severity. In line with this observation, children stratified according to ASD severity did not differ significantly in biochemical profiles at the group level, whereas correlation analyses revealed domain-specific associations between metabolic markers, immune parameters, and discrete neurodevelopmental dimensions, supporting a dimensional interpretation of biological variability in ASD [54,55].

Within this framework, homocysteine emerged in our data as a relevant metabolic marker, showing significant negative correlations with language and performance quotients on the GMDS-ER, while not distinguishing severity-based ASD subgroups. In addition, when analysed categorically, out-of-range homocysteine values were positively associated with restricted and repetitive behaviours. These findings are consistent with previous studies reporting altered homocysteine levels in ASD and related neurodevelopmental conditions, albeit with heterogeneous directionality across cohorts, suggesting that homocysteine may function as a state-dependent marker of metabolic efficiency rather than a uniform disease indicator [54,56,57]. The biological plausibility of this association is supported by the central role of homocysteine at the intersection of folate and vitamin B12 metabolism, methyl-group availability, and redox balance, which are processes repeatedly implicated in neurodevelopmental vulnerability [58,59].

Consistent with this interpretation, folate levels in our cohort showed positive correlations with motor and coordination quotients, suggesting that variability in folate-dependent metabolic pathways may preferentially influence motor development rather than ASD severity per se. Previous clinical and epidemiological studies have shown that folate availability modulates neurodevelopmental outcomes through its role in nucleotide synthesis and methylation reactions, and that functional effects may be detectable even in the absence of overt deficiency [54,60]. Large cohort studies further indicate that folate-related metabolic status is associated with specific developmental domains, supporting the relevance of domain-level analyses such as those applied in the present work [60].

Vitamin C also demonstrated domain-specific associations in our data, with lower levels correlating with increased tactile sensory alterations. This finding aligns with literature indicating that vitamin C contributes to neurodevelopment through antioxidant activity, modulation of neurotransmitter synthesis, and support of myelination, and that variability in antioxidant capacity may be reflected in sensory processing phenotypes rather than in global ASD severity [54,61].

Vitamin D showed a distinct and internally consistent pattern of associations, with positive correlations observed with oral and vestibular sensory profiles and negative correlations with auditory sensory responsivity. This sensory-specific mapping is

coherent with evidence that vitamin D plays a role in brain development and neuroimmune regulation, and that its effects in ASD are more consistently linked to behavioural and sensory dimensions than to diagnostic severity [56,59]. These findings support the interpretation that vitamin D status may modulate particular neurodevelopmental domains, potentially through immunomodulatory or neuromodulatory mechanisms, rather than acting as a nonspecific biomarker of ASD burden.

The immune findings in our cohort further reinforce a domain-oriented biological signal. Markers such as CRP, ESR, IgA, and IgM were selectively associated with sensory responsivity and behavioural organisation, without indicating a state of overt systemic inflammation. This pattern is consistent with early and subsequent studies suggesting that immune alterations in ASD are characterised by altered immune responsiveness or regulation rather than by chronic inflammatory activation [60,62]. Importantly, immune dysregulation in ASD has been shown to depend on both basal immune status and responsiveness to stimulation, highlighting the limitations of single time-point peripheral measurements [62].

Taken together, the present biochemical findings support the existence of metabolic–immune endophenotypic axes in ASD, characterised by variability in one-carbon metabolism (homocysteine and folate), vitamin-dependent and antioxidant pathways

(vitamins C and D), and low-grade immune markers. Crucially, these axes map onto specific developmental, sensory, and behavioural domains rather than onto overall ASD severity, reinforcing a dimensional model of biological heterogeneity consistent with integrative metabolic and immunological frameworks [58,63].

In the present cohort, structural brain MRI did not reveal ASD-specific abnormalities and was primarily employed to exclude major structural or syndromic conditions. This finding is consistent with extensive neuroimaging literature indicating that conventional structural MRI lacks a reproducible ASD-specific signature, while group-level structural differences are highly heterogeneous, developmentally dynamic, and not suitable as individual biomarkers [64,65].

In contrast, functional approaches appear more sensitive to ASD-related neurobiological alterations. In line with this framework, the EEG abnormalities observed in a subset of children in our cohort— including epileptiform activity and background rhythm alterations in the absence of clinical epilepsy—are consistent with evidence that ASD is characterized by atypical functional brain organization and network-level dysregulation rather than focal structural pathology [66].

Taken together, the findings of this thesis support the delineation of several converging endophenotypic dimensions in ASD. In particular, a redox–metabolic axis is suggested by the convergence of genetic vulnerability, oxidative stress markers, and domain-specific

metabolic–developmental associations, while an immune–regulatory dimension is indicated by epigenetic modulation of innate immune pathways and the selective relationships between inflammatory markers and sensory–behavioural profiles. In parallel, epigenetic alterations affecting synaptic and chromatin-related pathways, together with functional neurophysiological abnormalities, point toward a synaptic–neurodevelopmental dimension that intersects with early regulatory and sensory–motor traits.

These interpretations must nonetheless be approached with caution. Although biologically informative, the present dataset is limited by sample size in selected sub-analyses, by its cross-sectional design, and by the use of peripheral biomarkers as indirect proxies of central processes. As a result, the identified associations likely reflect vulnerability patterns or compensatory mechanisms rather than definitive mechanistic pathways, and robust individual-level stratification will require larger, longitudinal, multi-omic datasets.

Despite these limitations, this work contributes to the understanding of ASD heterogeneity by providing empirical evidence that biological variation in ASD is structured, non-random, and aligned with specific developmental and behavioural profiles. By demonstrating the feasibility of integrating genetic, epigenetic, biochemical, neurophysiological, and clinical data in children, this thesis supports a shift from

categorical toward stratified models of autism and highlights redox regulation, immune competence, synaptic development, and sensory–motor organisation as promising domains for early biological stratification.

8. Conclusions

This thesis supports the view that biological heterogeneity in autism spectrum disorder is best addressed through integrative and stratified frameworks rather than categorical models. The multidimensional approach adopted here demonstrates that meaningful biological signal can be captured in early childhood by jointly analysing genetic, epigenetic, metabolic, immune, and neurophysiological dimensions, even in the absence of robust severity-based group differences [49,67]. However, given the heterogeneity of data emerging from this study and the literature, a clear correlation between biological markers and clinical phenotypes is yet to be established, and the clinical evaluation remains at the moment the primary predictor of developmental trajectories.

Future research should prioritise longitudinal designs capable of tracking the developmental stability and temporal dynamics of biologically defined vulnerability domains, particularly during critical windows of neurodevelopment [68]. Integrating multi-omic data with functional readouts such as EEG and refined clinical phenotyping

will be essential to move from associative findings toward clinically meaningful stratification [66,69].

In this context, domains related to redox regulation, immune modulation, synaptic development, and sensory–motor organisation emerge as promising targets for early biological stratification and hypothesis-driven intervention studies, provided that future efforts incorporate adequate sample sizes, harmonised methodologies, and computational approaches to individual-level integration. Emerging interventional evidence suggests that antioxidant and metabolic-targeted approaches may exert modest but domain-specific effects on behavioural and communication outcomes in selected subgroups of autistic individuals, supporting the rationale for biologically informed, stratified treatment strategies rather than uniform therapeutic models [70].

Ultimately, the translation of ASD research toward precision-oriented models will depend on the ability to operationalise biologically informed endophenotypes into reproducible and developmentally sensitive frameworks, bridging molecular mechanisms and early clinical trajectories.

References

1. Lord, C.; Elsabbagh, M.; Baird, G.; Veenstra-Vanderweele, J. Autism Spectrum Disorder. Lancet Lond. Engl. 2018, 392, 508–520, doi:10.1016/S0140-6736(18)31129-2.

2. Maenner, M.J. Prevalence and Characteristics of Autism Spectrum Disorder Among Children Aged 8 Years — Autism and Developmental Disabilities Monitoring Network, 11 Sites, United States, 2020. MMWR Surveill. Summ. 2023, 72, doi:10.15585/mmwr.ss7202a1.
3. Hansen, S.N.; Schendel, D.E.; Parner, E.T. Explaining the Increase in the Prevalence of Autism Spectrum Disorders: The Proportion Attributable to Changes in Reporting Practices. JAMA Pediatr. 2015, 169, 56–62, doi:10.1001/jamapediatrics.2014.1893.
4. Lyall, K.; Schmidt, R.J.; Hertz-Picciotto, I. Maternal Lifestyle and Environmental Risk Factors for Autism Spectrum Disorders. Int. J. Epidemiol. 2014, 43, 443–464, doi:10.1093/ije/dyt282.
5. Hagerman, R.; Hoem, G.; Hagerman, P. Fragile X and Autism: Intertwined at the Molecular Level Leading to Targeted Treatments. Mol. Autism 2010, 1, 12, doi:10.1186/2040-2392-1-12.
6. Satterstrom, F.K.; Kosmicki, J.A.; Wang, J.; Breen, M.S.; De Rubeis, S.; An, J.-Y.; Peng, M.; Collins, R.; Grove, J.; Klei, L.; et al. Large-Scale Exome Sequencing Study Implicates Both Developmental and Functional Changes in the Neurobiology of Autism. Cell 2020, 180, 568-584.e23, doi:10.1016/j.cell.2019.12.036.
7. Paulsen, B.; Velasco, S.; Kedaigle, A.J.; Pigoni, M.; Quadrato, G.; Deo, A.J.; Adiconis, X.; Uzquiano, A.; Sartore, R.; Yang, S.M.; et al. Autism Genes Converge on Asynchronous Development of Shared Neuron Classes. Nature 2022, 602, 268–273, doi:10.1038/s41586-021-04358-6.
8. Willsey, H.R.; Willsey, A.J.; Wang, B.; State, M.W. Genomics, Convergent Neuroscience and Progress in Understanding Autism Spectrum Disorder. Nat. Rev. Neurosci. 2022, 23, 323–341, doi:10.1038/s41583-022-00576-7.
9. Wang, M.; Zhang, X.; Zhong, L.; Zeng, L.; Li, L.; Yao, P. Understanding Autism: Causes, Diagnosis, and Advancing Therapies. Brain Res. Bull. 2025, 227, 111411, doi:10.1016/j.brainresbull.2025.111411.
10. Zou, Y.; Lu, Q.; Zheng, D.; Chu, Z.; Liu, Z.; Chen, H.; Ruan, Q.; Ge, X.; Zhang, Z.; Wang, X.; et al. Prenatal Levonorgestrel Exposure Induces Autism-like Behavior in Offspring through ERβ Suppression in the Amygdala. Mol. Autism 2017, 8, 46, doi:10.1186/s13229-017-0159-3.

11. Baron-Cohen, S.; Tsompanidis, A.; Auyeung, B.; Nørgaard-Pedersen, B.; Hougaard, D.M.; Abdallah, M.; Cohen, A.; Pohl, A. Foetal Oestrogens and Autism. Mol. Psychiatry 2020, 25, 2970–2978, doi:10.1038/s41380-019-0454-9.
12. Tsamantioti, E.; Lisonkova, S.; Muraca, G.; Örtqvist, A.K.; Razaz, N. Chorioamnionitis and Risk of Long-Term Neurodevelopmental Disorders in Offspring: A Population-Based Cohort Study. Am. J. Obstet. Gynecol. 2022, 227, 287.e1-287.e17, doi:10.1016/j.ajog.2022.03.028.
13. Tartaglione, A.M.; Camoni, L.; Calamandrei, G.; Chiarotti, F.; Venerosi, A. The Contribution of Environmental Pollutants to the Risk of Autism and Other Neurodevelopmental Disorders: A Systematic Review of Case-Control Studies. Neurosci. Biobehav. Rev. 2024, 164, 105815, doi:10.1016/j.neubiorev.2024.105815.
14. Masini, E.; Loi, E.; Vega-Benedetti, A.F.; Carta, M.; Doneddu, G.; Fadda, R.; Zavattari, P. An Overview of the Main Genetic, Epigenetic and Environmental Factors Involved in Autism Spectrum Disorder Focusing on Synaptic Activity. Int. J. Mol. Sci. 2020, 21, 8290, doi:10.3390/ijms21218290.
15. Denomme, M.M.; Haywood, M.E.; Parks, J.C.; Schoolcraft, W.B.; Katz-Jaffe, M.G. The Inherited Methylome Landscape Is Directly Altered with Paternal Aging and Associated with Offspring Neurodevelopmental Disorders. Aging Cell 2020, 19, e13178, doi:10.1111/acel.13178.
16. Lord, C.; Brugha, T.S.; Charman, T.; Cusack, J.; Dumas, G.; Frazier, T.; Jones, E.J.H.; Jones, R.M.; Pickles, A.; State, M.W.; et al. Autism Spectrum Disorder. Nat. Rev. Dis. Primer 2020, 6, 5, doi:10.1038/s41572-019-0138-4.
17. Cortese, S.; Solmi, M.; Michelini, G.; Bellato, A.; Blanner, C.; Canozzi, A.; Eudave, L.; Farhat, L.C.; Højlund, M.; Köhler-Forsberg, O.; et al. Candidate Diagnostic Biomarkers for Neurodevelopmental Disorders in Children and Adolescents: A Systematic Review. World Psychiatry Off. J. World Psychiatr. Assoc. WPA 2023, 22, 129–149, doi:10.1002/wps.21037.
18. Liu, J.; Tan, Y.; Zhang, F.; Wang, Y.; Chen, S.; Zhang, N.; Dai, W.; Zhou, L.; Li, J.-C. Metabolomic Analysis of Plasma Biomarkers in Children with Autism Spectrum Disorders. MedComm 2024, 5, e488, doi:10.1002/mco2.488.

19. Moreno, R.J.; Rose, D.R.; Tancredi, D.J.; Schmidt, R.J.; Ozonoff, S.J.; Ashwood, P. Cord Blood Cytokine Profiles in Children Later Diagnosed with Autism Spectrum Disorder: Results from the Prospective MARBLES Study. Brain. Behav. Immun. 2024, 122, 339–344, doi:10.1016/j.bbi.2024.08.036.
20. Gottesman, I.I.; Gould, T.D. The Endophenotype Concept in Psychiatry: Etymology and Strategic Intentions. Am. J. Psychiatry 2003, 160, 636–645, doi:10.1176/appi.ajp.160.4.636.
21. Lombardo, M.V.; Lai, M.-C.; Baron-Cohen, S. Big Data Approaches to Decomposing Heterogeneity across the Autism Spectrum. Mol. Psychiatry 2019, 24, 1435–1450, doi:10.1038/s41380-018-0321-0.
22. American Psychiatric Association; American Psychiatric Association DSM-5 Task Force Diagnostic and Statistical Manual of Mental Disorders: DSM-5; 5th ed.; Washington, D.C.: American Psychiatric Association: United States, 2013; ISBN 978-0-89042-554-1.
23. Alagozlu, H.; Gorgul, A.; Bilgihan, A.; Tuncer, C.; Unal, S. Increased Plasma Levels of Advanced Oxidation Protein Products (AOPP) as a Marker for Oxidative Stress in Patients with Active Ulcerative Colitis. Clin. Res. Hepatol. Gastroenterol. 2013, 37, 80–85, doi:10.1016/j.clinre.2012.03.034.
24. Collins, A.R. The Comet Assay for DNA Damage and Repair: Principles, Applications, and Limitations. Mol. Biotechnol. 2004, 26, 249–261, doi:10.1385/MB:26:3:249.
25. Olive, P.L.; Banáth, J.P. The Comet Assay: A Method to Measure DNA Damage in Individual Cells. Nat. Protoc. 2006, 1, 23–29, doi:10.1038/nprot.2006.5.
26. Gugliandolo, A.; Gangemi, C.; Calabrò, C.; Vecchio, M.; Di Mauro, D.; Renis, M.; Ientile, R.; Currò, M.; Caccamo, D. Assessment of Glutathione Peroxidase-1 Polymorphisms, Oxidative Stress and DNA Damage in Sensitivity-Related Illnesses. Life Sci. 2016, 145, 27–33, doi:10.1016/j.lfs.2015.12.028.
27. Frustaci, A.; Neri, M.; Cesario, A.; Adams, J.B.; Domenici, E.; Dalla Bernardina, B.; Bonassi, S. Oxidative Stress-Related Biomarkers in Autism: Systematic Review and Meta-Analyses. Free Radic. Biol. Med. 2012, 52, 2128–2141, doi:10.1016/j.freeradbiomed.2012.03.011.

28. Liu, X.; Lin, J.; Zhang, H.; Khan, N.U.; Zhang, J.; Tang, X.; Cao, X.; Shen, L. Oxidative Stress in Autism Spectrum Disorder-Current Progress of Mechanisms and Biomarkers. Front. Psychiatry 2022, 13, 813304, doi:10.3389/fpsyt.2022.813304.
29. Rossignol, D.A.; Frye, R.E. Evidence Linking Oxidative Stress, Mitochondrial Dysfunction, and Inflammation in the Brain of Individuals with Autism. Front. Physiol. 2014, 5, 150, doi:10.3389/fphys.2014.00150.
30. Bjørklund, G.; Tinkov, A.A.; Hosnedlová, B.; Kizek, R.; Ajsuvakova, O.P.; Chirumbolo, S.; Skalnaya, M.G.; Peana, M.; Dadar, M.; El-Ansary, A.; et al. The Role of Glutathione Redox Imbalance in Autism Spectrum Disorder: A Review. Free Radic. Biol. Med. 2020, 160, 149–162, doi:10.1016/j.freeradbiomed.2020.07.017.
31. Shao, X.; Yan, C.; Sun, D.; Fu, C.; Tian, C.; Duan, L.; Zhu, G. Association Between Glutathione Peroxidase-1 (GPx-1) Polymorphisms and Schizophrenia in the Chinese Han Population. Neuropsychiatr. Dis. Treat. 2020, 16, 2297–2305, doi:10.2147/NDT.S272278.
32. Banhela, N.; Naidoo, P.; Naidoo, S. Association between Pesticide Exposure and Paraoxonase-1 (PON1) Polymorphisms, and Neurobehavioural Outcomes in Children: A Systematic Review. Syst. Rev. 2020, 9, 109, doi:10.1186/s13643-020-01330-9.
33. Gaita, L.; Manzi, B.; Sacco, R.; Lintas, C.; Altieri, L.; Lombardi, F.; Pawlowski, T.L.; Redman, M.; Craig, D.W.; Huentelman, M.J.; et al. Decreased Serum Arylesterase Activity in Autism Spectrum Disorders. Psychiatry Res. 2010, 180, 105–113, doi:10.1016/j.psychres.2010.04.010.
34. Volk, H.E.; Ames, J.L.; Chen, A.; Fallin, M.D.; Hertz-Picciotto, I.; Halladay, A.; Hirtz, D.; Lavin, A.; Ritz, B.; Zoeller, T.; et al. Considering Toxic Chemicals in the Etiology of Autism. Pediatrics 2022, 149, e2021053012, doi:10.1542/peds.2021-053012.
35. Yenkoyan, K.; Harutyunyan, H.; Harutyunyan, A. A Certain Role of SOD/CAT Imbalance in Pathogenesis of Autism Spectrum Disorders. Free Radic. Biol. Med. 2018, 123, 85–95, doi:10.1016/j.freeradbiomed.2018.05.070.
36. Kovač, J.; Macedoni Lukšič, M.; Trebušak Podkrajšek, K.; Klančar, G.; Battelino, T. Rare Single Nucleotide Polymorphisms in the Regulatory Regions of the Superoxide Dismutase Genes in Autism Spectrum Disorder. Autism Res. Off. J. Int. Soc. Autism Res. 2014, 7, 138–144, doi:10.1002/aur.1345.

37. Esparham, A.E.; Smith, T.; Belmont, J.M.; Haden, M.; Wagner, L.E.; Evans, R.G.; Drisko, J.A. Nutritional and Metabolic Biomarkers in Autism Spectrum Disorders: An Exploratory Study. Integr. Med. Encinitas Calif 2015, 14, 40–53.
38. Tanner, S.; Thomson, S.; Drummond, K.; O'Hely, M.; Symeonides, C.; Mansell, T.; Saffery, R.; Sly, P.D.; Collier, F.; Burgner, D.; et al. A Pathway-Based Genetic Score for Oxidative Stress: An Indicator of Host Vulnerability to Phthalate-Associated Adverse Neurodevelopment. Antioxid. Basel Switz. 2022, 11, 659, doi:10.3390/antiox11040659.
39. Manivasagam, T.; Arunadevi, S.; Essa, M.M.; SaravanaBabu, C.; Borah, A.; Thenmozhi, A.J.; Qoronfleh, M.W. Role of Oxidative Stress and Antioxidants in Autism. Adv. Neurobiol. 2020, 24, 193–206, doi:10.1007/978-3-030-30402-7_7.
40. Mandic-Maravic, V.; Mitkovic-Voncina, M.; Pljesa-Ercegovac, M.; Savic-Radojevic, A.; Djordjevic, M.; Ercegovac, M.; Pekmezovic, T.; Simic, T.; Pejovic-Milovancevic, M. Glutathione S-Transferase Polymorphisms and Clinical Characteristics in Autism Spectrum Disorders. Front. Psychiatry 2021, 12, 672389, doi:10.3389/fpsyt.2021.672389.
41. Morales, E.; Sunyer, J.; Castro-Giner, F.; Estivill, X.; Julvez, J.; Ribas-Fitó, N.; Torrent, M.; Grimalt, J.O.; de Cid, R. Influence of Glutathione S-Transferase Polymorphisms on Cognitive Functioning Effects Induced by p,p'-DDT among Preschoolers. Environ. Health Perspect. 2008, 116, 1581–1585, doi:10.1289/ehp.11303.
42. Youngster, I.; Zachor, D.A.; Gabis, L.V.; Bar-Chaim, A.; Benveniste-Levkovitz, P.; Britzi, M.; Soback, S.; Ziv-Baran, T.; Berkovitch, M. CYP2D6 Genotyping in Paediatric Patients with Autism Treated with Risperidone: A Preliminary Cohort Study. Dev. Med. Child Neurol. 2014, 56, 990–994, doi:10.1111/dmcn.12470.
43. Vanwong, N.; Ngamsamut, N.; Medhasi, S.; Puangpetch, A.; Chamnanphon, M.; Tan-Kam, T.; Hongkaew, Y.; Limsila, P.; Sukasem, C. Impact of CYP2D6 Polymorphism on Steady-State Plasma Levels of Risperidone and 9-Hydroxyrisperidone in Thai Children and Adolescents with Autism Spectrum Disorder. J. Child Adolesc. Psychopharmacol. 2017, 27, 185–191, doi:10.1089/cap.2014.0171.

44. Biswas, M.; Vanwong, N.; Sukasem, C. Pharmacogenomics in Clinical Practice to Prevent Risperidone-Induced Hyperprolactinemia in Autism Spectrum Disorder. Pharmacogenomics 2022, 23, 493–503, doi:10.2217/pgs-2022-0016.
45. Horinouchi, T.; Maeyama, K.; Nagai, M.; Mizobuchi, M.; Takagi, Y.; Okada, Y.; Kato, T.; Nishimura, M.; Kawasaki, Y.; Yoshioka, M.; et al. Genetic Analysis of UGT1A1 Polymorphisms Using Preserved Dried Umbilical Cord for Assessing the Potential of Neonatal Jaundice as a Risk Factor for Autism Spectrum Disorder in Children. J. Autism Dev. Disord. 2022, 52, 483–489, doi:10.1007/s10803-021-04941-w.
46. Morimoto, M.; Hashimoto, T.; Tsuda, Y.; Nakatsu, T.; Kitaoka, T.; Kyotani, S. Assessment of Oxidative Stress in Autism Spectrum Disorder Using Reactive Oxygen Metabolites and Biological Antioxidant Potential. PloS One 2020, 15, e0233550, doi:10.1371/journal.pone.0233550.
47. Ladd-Acosta, C.; Hansen, K.D.; Briem, E.; Fallin, M.D.; Kaufmann, W.E.; Feinberg, A.P. Common DNA Methylation Alterations in Multiple Brain Regions in Autism. Mol. Psychiatry 2014, 19, 862–871, doi:10.1038/mp.2013.114.
48. Forsberg, S.L.; Ilieva, M.; Maria Michel, T. Epigenetics and Cerebral Organoids: Promising Directions in Autism Spectrum Disorders. Transl. Psychiatry 2018, 8, 14, doi:10.1038/s41398-017-0062-x.
49. Williams, L.A.; LaSalle, J.M. Future Prospects for Epigenetics in Autism Spectrum Disorder. Mol. Diagn. Ther. 2022, 26, 569–579, doi:10.1007/s40291-022-00608-z.
50. Mordaunt, C.E.; Jianu, J.M.; Laufer, B.I.; Zhu, Y.; Hwang, H.; Dunaway, K.W.; Bakulski, K.M.; Feinberg, J.I.; Volk, H.E.; Lyall, K.; et al. Cord Blood DNA Methylome in Newborns Later Diagnosed with Autism Spectrum Disorder Reflects Early Dysregulation of Neurodevelopmental and X-Linked Genes. Genome Med. 2020, 12, 88, doi:10.1186/s13073-020-00785-8.
51. Massrali, A.; Brunel, H.; Hannon, E.; Wong, C.; iPSYCH-MINERvA Epigenetics Group; Baron-Cohen, S.; Warrier, V. Integrated Genetic and Methylomic Analyses Identify Shared Biology between Autism and Autistic Traits. Mol. Autism 2019, 10, 31, doi:10.1186/s13229-019-0279-z.
52. Kushak, R.I.; Sengupta, A.; Winter, H.S. Interactions between the Intestinal Microbiota and Epigenome in Individuals with Autism Spectrum Disorder. Dev. Med. Child Neurol. 2022, 64, 296–304, doi:10.1111/dmcn.15052.

53. Tisato, V.; Silva, J.A.; Longo, G.; Gallo, I.; Singh, A.V.; Milani, D.; Gemmati, D. Genetics and Epigenetics of One-Carbon Metabolism Pathway in Autism Spectrum Disorder: A Sex-Specific Brain Epigenome? Genes 2021, 12, 782, doi:10.3390/genes12050782.
54. Adams, J.B.; George, F.; Audhya, T. Abnormally High Plasma Levels of Vitamin B6 in Children with Autism Not Taking Supplements Compared to Controls Not Taking Supplements. J. Altern. Complement. Med. N. Y. N 2006, 12, 59–63, doi:10.1089/acm.2006.12.59.
55. Gevi, F.; Zolla, L.; Gabriele, S.; Persico, A.M. Urinary Metabolomics of Young Italian Autistic Children Supports Abnormal Tryptophan and Purine Metabolism. Mol. Autism 2016, 7, 47, doi:10.1186/s13229-016-0109-5.
56. Saha, S.; Saha, T.; Sinha, S.; Rajamma, U.; Mukhopadhyay, K. Autistic Traits and Components of the Folate Metabolic System: An Explorative Analysis in the Eastern Indian ASD Subjects. Nutr. Neurosci. 2020, 23, 860–867, doi:10.1080/1028415X.2019.1570442.
57. Chen, W.-X.; Chen, Y.-R.; Peng, M.-Z.; Liu, X.; Cai, Y.-N.; Huang, Z.-F.; Yang, S.-Y.; Huang, J.-Y.; Wang, R.-H.; Yi, P.; et al. Plasma Amino Acid Profile in Children with Autism Spectrum Disorder in Southern China: Analysis of 110 Cases. J. Autism Dev. Disord. 2024, 54, 1567–1581, doi:10.1007/s10803-022-05829-z.
58. Belardo, A.; Gevi, F.; Zolla, L. The Concomitant Lower Concentrations of Vitamins B6, B9 and B12 May Cause Methylation Deficiency in Autistic Children. J. Nutr. Biochem. 2019, 70, 38–46, doi:10.1016/j.jnutbio.2019.04.004.
59. Li, H.; Dang, Y.; Yan, Y. Serum Interleukin-17 A and Homocysteine Levels in Children with Autism. BMC Neurosci. 2024, 25, 17, doi:10.1186/s12868-024-00860-5.
60. Krakowiak, P.; Goines, P.E.; Tancredi, D.J.; Ashwood, P.; Hansen, R.L.; Hertz-Picciotto, I.; Van de Water, J. Neonatal Cytokine Profiles Associated With Autism Spectrum Disorder. Biol. Psychiatry 2017, 81, 442–451, doi:10.1016/j.biopsych.2015.08.007.
61. Altun, H.; Kurutaş, E.B.; Şahin, N.; Güngör, O.; Fındıklı, E. The Levels of Vitamin D, Vitamin D Receptor, Homocysteine and Complex B Vitamin in Children with Autism Spectrum Disorders. Clin. Psychopharmacol. Neurosci. Off. Sci. J. Korean Coll. Neuropsychopharmacol. 2018, 16, 383–390, doi:10.9758/cpn.2018.16.4.383.

62. Croonenberghs, J.; Bosmans, E.; Deboutte, D.; Kenis, G.; Maes, M. Activation of the Inflammatory Response System in Autism. Neuropsychobiology 2002, 45, 1–6, doi:10.1159/000048665.
63. Carpita, B.; Massoni, L.; Battaglini, S.; Palego, L.; Cremone, I.M.; Massimetti, G.; Betti, L.; Giannaccini, G.; Dell'Osso, L. IL-6, Homocysteine, and Autism Spectrum Phenotypes: An Investigation among Adults with Autism Spectrum Disorder and Their First-Degree Relatives. CNS Spectr. 2023, 28, 620–628, doi:10.1017/S1092852923000019.
64. Rafiee, F.; Rezvani Habibabadi, R.; Motaghi, M.; Yousem, D.M.; Yousem, I.J. Brain MRI in Autism Spectrum Disorder: Narrative Review and Recent Advances. J. Magn. Reson. Imaging JMRI 2022, 55, 1613–1624, doi:10.1002/jmri.27949.
65. Ecker, C.; Bookheimer, S.Y.; Murphy, D.G.M. Neuroimaging in Autism Spectrum Disorder: Brain Structure and Function across the Lifespan. Lancet Neurol. 2015, 14, 1121–1134, doi:10.1016/S1474-4422(15)00050-2.
66. O'Reilly, C.; Lewis, J.D.; Elsabbagh, M. Is Functional Brain Connectivity Atypical in Autism? A Systematic Review of EEG and MEG Studies. PloS One 2017, 12, e0175870, doi:10.1371/journal.pone.0175870.
67. Havdahl, K.A.; Hus Bal, V.; Huerta, M.; Pickles, A.; Øyen, A.-S.; Stoltenberg, C.; Lord, C.; Bishop, S.L. Multidimensional Influences on Autism Symptom Measures: Implications for Use in Etiological Research. J. Am. Acad. Child Adolesc. Psychiatry 2016, 55, 1054-1063.e3, doi:10.1016/j.jaac.2016.09.490.
68. Hadders-Algra, M. Early Diagnostics and Early Intervention in Neurodevelopmental Disorders-Age-Dependent Challenges and Opportunities. J. Clin. Med. 2021, 10, 861, doi:10.3390/jcm10040861.
69. Lim, L.; Chantiluke, K.; Cubillo, A.I.; Smith, A.B.; Simmons, A.; Mehta, M.A.; Rubia, K. Disorder-Specific Grey Matter Deficits in Attention Deficit Hyperactivity Disorder Relative to Autism Spectrum Disorder. Psychol. Med. 2015, 45, 965–976, doi:10.1017/S0033291714001974.
70. Liu, Y.; Yang, Z.; Du, Y.; Shi, S.; Cheng, Y. Antioxidant Interventions in Autism Spectrum Disorders: A Meta-Analysis. Prog. Neuropsychopharmacol. Biol. Psychiatry 2022, 113, 110476, doi:10.1016/j.pnpbp.2021.110476.